

A FINITE ELEMENT STUDY  
ON THE EFFECTIVE WIDTH OF FLANGED SECTIONS

A THESIS SUBMITTED TO  
THE GRADUATE SCHOOL OF NATURAL AND APPLIED SCIENCES  
OF  
MIDDLE EAST TECHNICAL UNIVERSITY

BY

SERTAÇ KÜÇÜKARSLAN

IN PARTIAL FULFILLMENT OF THE REQUIREMENTS  
FOR  
THE DEGREE OF MASTER OF SCIENCE  
IN  
CIVIL ENGINEERING

JULY 2010

Approval of the thesis:

**A FINITE ELEMENT STUDY  
ON THE EFFECTIVE WIDTH OF FLANGED SECTIONS**

submitted by **SERTAÇ KÜÇÜKARSLAN** in partial fulfillment of the requirements for the degree of **Master of Science in Civil Engineering Department, Middle East Technical University** by,

Prof. Dr. Canan Özgen  
Dean, Graduate School of **Natural and Applied Sciences**

Prof. Dr. Güney Özcebe  
Head of Department, **Civil Engineering**

Prof. Dr. Mehmet Utku  
Supervisor, **Civil Engineering Dept., METU**

**Examining Committee Members:**

Prof. Dr. Sinan Altın  
Civil Engineering Dept., Gazi University

Prof. Dr. Mehmet Utku  
Civil Engineering Dept., METU

Assoc. Prof. Dr. Uğur Polat  
Civil Engineering Dept., METU

Asst. Prof. Dr. Ayşegül Askan Gündoğan  
Civil Engineering Dept., METU

Asst. Prof. Dr. Afşin Sarıtaş  
Civil Engineering Dept., METU

**Date:** 07.07.2010

**I hereby declare that all information in this document has been obtained and presented in accordance with academic rules and ethical conduct. I also declare that, as required by these rules and conduct, I have fully cited and referenced all material and results that are not original to this work.**

Name, Last name : Sertaç Küçükarslan

Signature :

# **ABSTRACT**

## **A FINITE ELEMENT STUDY ON THE EFFECTIVE WIDTH OF FLANGED SECTIONS**

Küçükarslan, Sertaç

M.Sc., Department of Civil Engineering

Supervisor: Prof. Dr. Mehmet Utku

July 2010, 63 pages

Most of the reinforced concrete systems are monolithic. During construction, concrete from the bottom of the deepest beam to the top of slab, is placed at once. Therefore the slab serves as the top flange of the beams. Such a beam is referred to as T-beam. In a floor system made of T-beams, the compressive stress is a maximum over the web, dropping between the webs. The distribution of compressive stress on the flange depends on the relative dimensions of the cross section, span length, support and loading conditions. For simplification, the varying distribution of compressive stress can be replaced by an equivalent uniform distribution. This gives us an effective flange width, which is smaller than the real flange width. In various codes there are recommendations for effective flange width formulas. But these formulas are expressed only in terms of span length or flange and web thicknesses and ignore the other important variables.

In this thesis, three-dimensional finite element analysis has been carried out on continuous T-beams under different loading conditions to assess the effective flange width based on displacement criterion. The formulation is based on a combination of the elementary bending theory and the finite element method, accommodating partial interaction in between. The beam spacing, beam span length, total depth of the beam, the web and the flange thicknesses are considered as independent variables. Depending on the type of loading, the numerical value of the moment of inertia of the transformed beam cross-section and hence the effective flange width are calculated. The input data and the finite element displacement results are then used in a nonlinear regression analysis and two explicit design formulas for effective flange width have been derived. Comparisons are made between the proposed formulas and the ACI, Eurocode, TS-500 and BS-8110 code recommendations.

Keywords: Flange, Building Codes, T-beam, Compressive Stress, Effective Flange Width, Finite Element Analysis, Nonlinear Regression Analysis.

## ÖZ

### TABLALI KESİTLERİN ETKİLİ TABLA GENİŞLİĞİNİN SONLU ELEMENLAR YÖNTEMİ İLE ANALİZİ

Küçükarslan, Sertaç

Yüksek Lisans, İnşaat Mühendisliği Bölümü

Tez Yöneticisi: Prof. Dr. Mehmet Utku

Temmuz 2010, 63 sayfa

Çoğu betonarme sistemler monolitikdir. İnşa sırasında beton en derindeki kirişin altından, döşemenin üstüne kadar bir kerede dökülür. Bu yüzden döşeme, kirişlerin üst tablası gibi çalışır. Böyle kirişlere T-kiriş denir. T-kirişlerden oluşmuş döşeme sistemlerinde basınç gerilimi kiriş gövdesi üzerinde maksimum olup, gövde aralarında düşer. Tabla üzerindeki basınç gerilimi dağılımı kesit boyutlarına, kiriş açıklığına, mesnet ve yükleme koşullarına bağlıdır. Basitleştirmek için değişen basınç gerilimi dağılımı eşdeğer düzgün dağılımla yer değiştirilebilir. Bu bize gerçek tabla genişliğinden daha küçük olan etkili tabla genişliğini verir. Çeşitli yönetmeliklerde etkili tabla genişliği formülleri için öneriler mevcuttur. Ancak bu formüller diğer önemli değişkenler ihmal edilerek, sadece kiriş açıklığı veya gövde ve tabla kalınlıkları cinsinden ifade edilmişlerdir.

Bu çalışmada, deplasmana dayalı etkili tabla genişliğinin belirlenmesi için sürekli T-kirişlerin üç boyutlu sonlu elemanlar analizi gerçekleştirilmiştir. Formülasyon, basit eğilme teorisi ile sonlu elemanlar methodunun kısmi

etkileşimine dayanmaktadır. Kirişler arasındaki uzaklık, kiriş açıklığı, kiriş derinliği, tabla ve gövde kalınlığı bağımsız değişkenler olarak alınmıştır. Sonlu elemanlar analizinden elde edilen desplasman değerleri kullanılarak, belirtilen değişkenlerin çeşitli değerleri için etkili tabla genişlikleri hesaplanmıştır. Yükleme durumuna bağlı olarak, dönüştürülmüş kiriş kesitinin atalet momenti ve dolayısıyla etkili tabla genişliği hesaplanmıştır. Veriler ve sonlu eleman deplasman sonuçları kullanılarak, doğrusal olmayan regresyon analizi yapılmış ve etkili tabla genişliği için açık tasarım formülleri türetilmiştir. Bu formüller ile ACI, Eurocode, TS-500 ve BS-8110 yönetmeliklerinin önerileri karşılaştırılmıştır.

Anahtar Kelimeler: Tabla, Yapı Yönetmelikleri, T-kiriş, Basınç Gerilimi, Etkili Tabla Genişliği, Sonlu Elemanlar Analizi, Doğrusal Olmayan Regresyon Analizi.

To My Wife

## **ACKNOWLEDGEMENTS**

The author wishes to express his deepest appreciation to his supervisor Prof. Dr. Mehmet UTKU for his guidance, criticism, encouragements and helpful advice throughout the research.

The author would also like to thank Prof. Dr. Semih YÜCEMEN for his suggestions and comments.

The author offers sincere thanks to his wife for her unshakable faith in him, her patience and confidence in him. She receives many indebted thanks.

# TABLE OF CONTENTS

<b>ABSTRACT .....</b>	<b>IV</b>
<b>ÖZ .....</b>	<b>VII</b>
<b>ACKNOWLEDGEMENTS.....</b>	<b>IX</b>
<b>TABLE OF CONTENTS.....</b>	<b>X</b>
<b>LIST OF TABLES .....</b>	<b>XIII</b>
<b>LIST OF FIGURES .....</b>	<b>XIII</b>
<b>LIST OF SYMBOLS .....</b>	<b>XV</b>
<b>CHAPTERS</b>	
<b>1. INTRODUCTION.....</b>	<b>1</b>
1.1. PRELIMINARY REMARKS .....	1
1.2. SURVEY OF PREVIOUS STUDIES.....	5
1.3. SCOPE OF THESIS .....	5
<b>2. EFFECTIVE FLANGE WIDTH AND CODE RECOMMENDATIONS.....</b>	<b>7</b>
2.1. CONCEPT OF EFFECTIVE FLANGE WIDTH.....	7
2.2. CODE RECOMMENDATIONS.....	9
2.2.1. ACI BUILDING CODE .....	9
2.2.2. EUROCODE.....	11
2.2.3. TS-500 .....	13
2.2.4. BRITISH STANDARDS BS-8110.....	14
<b>3. FORMULATION OF THE PROBLEM.....</b>	<b>15</b>
3.1. EFFECTIVE FLANGE WIDTH BASED ON DEFLECTION CRITERION .....	15
3.2. POINT LOAD AT MIDSPAN.....	15
3.3. UNIFORMLY DISTRIBUTED LOAD ON FLANGE.....	19
3.4. TRANSFORMED T-SECTION.....	22

<b>4. FINITE ELEMENT ANALYSIS.....</b>	<b>26</b>
4.1. THE SOLID ELEMENT .....	26
4.2. PARAMETERS INFLUENCING THE EFFECTIVE FLANGE WIDTH .....	28
4.3. FINITE ELEMENT MODEL .....	29
4.4. NUMERICAL STUDIES .....	36
<b>5. MULTIPLE NONLINEAR REGRESSION ANALYSIS .....</b>	<b>46</b>
5.1. MULTIPLE NONLINEAR REGRESSION .....	46
5.2. NONLINEAR REGRESSION MODEL .....	47
5.3. COMPARISON WITH THE CODE EQUATIONS .....	50
<b>6. CONCLUSIONS .....</b>	<b>60</b>
<b>REFERENCES.....</b>	<b>62</b>

## LIST OF TABLES

### TABLES

Table 2.1 Values for $\alpha$ .....	13
Table 4.1 Dimensionless parameters.....	29
Table 4.2 Effective flange width results for loading at midspan.....	38
Table 4.3 Effective flange width results for uniform loading .....	42
Table 5.1: Estimate values of parameters (Load at midspan).....	48
Table 5.2: Estimate values of parameters (Uniformly Distributed Load).....	49

## LIST OF FIGURES

### FIGURES

Figure 1.1: T-beams in a one-way slab floor.....	2
Figure 1.2: Typical cross-section and dimensions of a T-beam.....	2
Figure 1.3: Forces on a T-beam.....	3
Figure 1.4: Distribution of maximum flexural compressive stresses.....	4
Figure 1.5: Uniform stress distribution and “effective flange width”.....	4
Figure 2.1: Compressive stress block of T-section.....	8
Figure 2.2: Elevation showing definition of $l_0$ for calculation of flange width .....	11
Figure 2.3: Section showing effective flange width parameters .....	12
Figure 2.4: Definition of dimensions in T-beams.....	14
Figure 3.1: Load at midspan.....	16
Figure 3.2: Shear, moment, and deflection diagrams for load at midspan...	18
Figure 3.3: Uniformly distributed load.....	19
Figure 3.4: Shear, moment, and deflection diagrams for uniform loading....	21
Figure 3.5: Neutral axis passing through the web.....	22
Figure 3.6a: Part $A_1$ of the cross-section.....	23
Figure 3.6b: Part $A_2$ of the cross-section.....	23
Figure 3.6c: Part $A_3$ of the cross-section.....	23
Figure 3.7: Neutral axis passing through the flange.....	25
Figure 4.1a: Three-dimensional state of stress.....	26
Figure 4.1b: Eight-node solid element.....	26
Figure 4.1c: Degrees of freedom at a typical node ( $i= 1, 2... 8$ ).....	26

Figure 4.2: Eight-node isoparametric solid element.....	27
Figure 4.3: Dimensions of a T-beam.....	28
Figure 4.4: Longitudinal view of the finite element model.....	30
Figure 4.5a: Cross section of the finite element model.....	31
Figure 4.5b: Three dimensional finite element model.....	31
Figure 4.6: Flexural stress distribution for uniform loading.....	32
Figure 4.7: Deformed shape under uniform loading.....	33
Figure 4.8: Flexural stress distribution for loading at midspan.....	34
Figure 4.9: Deformed shape under loading at midspan.....	35
Figure 5.1: Comparison of design formulas with the code equations for load at midspan .....	50
Figure 5.2: “S/L” versus “ $b_e/S$ ” for Case1, Case2 and Case3.....	52
Figure 5.3: Effective flange width based on stress criterion and deflection consideration (Point load) .....	53
Figure 5.4: Comparison of design formulas with the code equations for uniformly distributed load .....	55
Figure 5.5: “S/L” versus “ $b_e/S$ ” for Case1, Case2 and Case3.....	57
Figure 5.6: Effective flange width based on stress criterion and deflection consideration (Uniform loading) .....	58

## LIST OF SYMBOLS

$a$	: Coefficient for determining zero moment distance of beam span.
$b_e, b_{eff}$	: Effective flange width
$h$	: Flange thickness of the beam
$S$	: Beam spacing between two adjacent beams
$D$	: Beam total depth
$L$	: Beam span length
$b_w$	: Web thickness of the beam
$\sigma_{ymax}$	: Maximum flexural stress
$l_0, l_z, l_p$	: Span length between two zero moment points
$v$	: Analytic displacement value
$v_{FE}$	: Displacement value based on finite element analysis
$E$	: Modulus of elasticity
$I$	: Moment of inertia of the beam
$f$	: A function of the covariate vector
$Y_i$	: Response
$\varepsilon$	: Random error

# CHAPTER 1

## INTRODUCTION

### 1.1. Preliminary Remarks

Reinforced concrete structural systems such as floors and roofs are almost monolithic, except precast systems. In a one-way beam-and-slab floor system, the slab is assumed to carry the loads in the direction perpendicular to the supporting beams. Under different service loading types, beams under slabs will have negative moment at support regions whereas they will have positive moment along unsupported span zone. This positive internal moment will cause compression in the upper part of the beam. Due to monolithic property of such systems where beam stirrups and top reinforcing bars of beams extend up into the slab, monolithically placed part of the slab and supporting beam will interact as a single unit in resisting the flexural compressive stresses caused by the positive moment. This results in a T-shaped beam cross section rather than a rectangular beam. Such a beam is referred to as a T-beam. The slab forms the beam flange while the part of the beam projecting below the slab forms the web. These details are described in such texts as Nilson and Winter (1991), Ersoy (1994) and MacGregor (2005). The typical monolithic structural system is shown in Figure 1.1 and a cross-section passing through such a T-beam defining the parameters is shown in Figure 1.2.

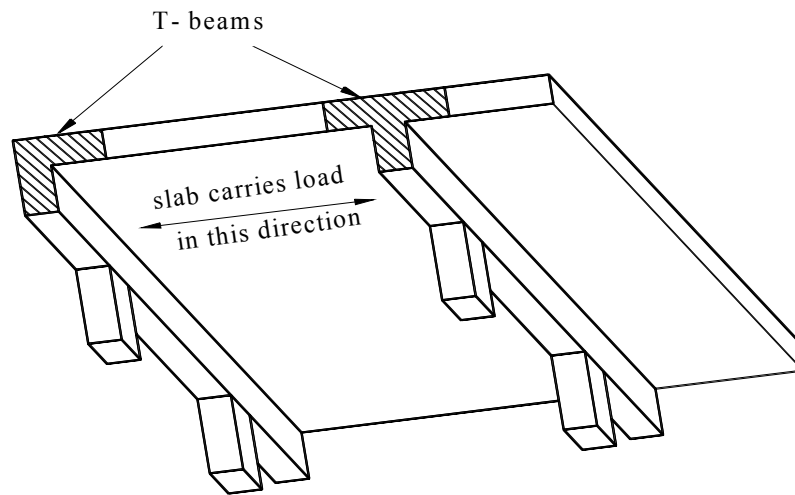


Figure 1.1 T-beams in a one-way slab floor (From MacGregor (2005))

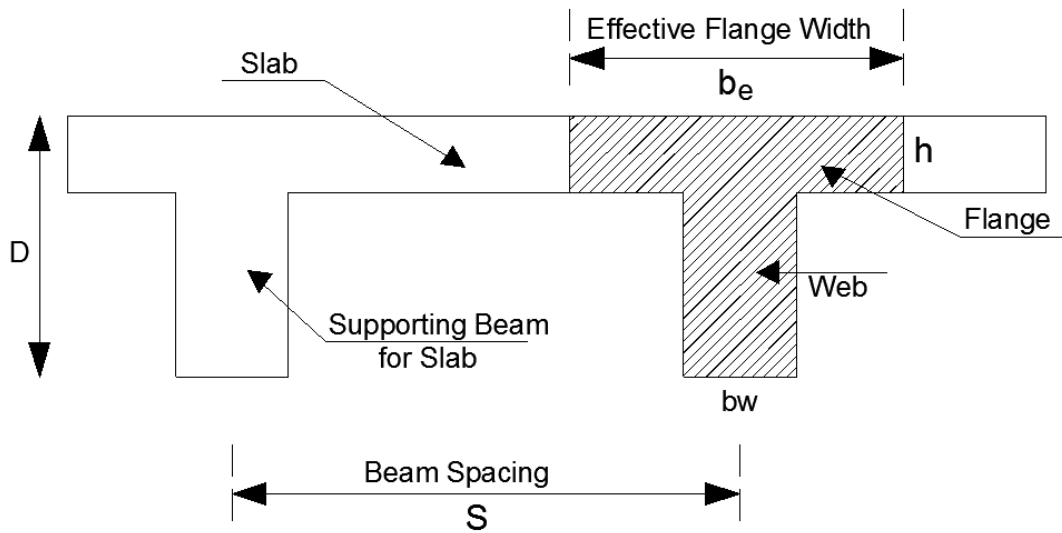


Figure 1.2 Typical cross-section and dimensions of a T-beam

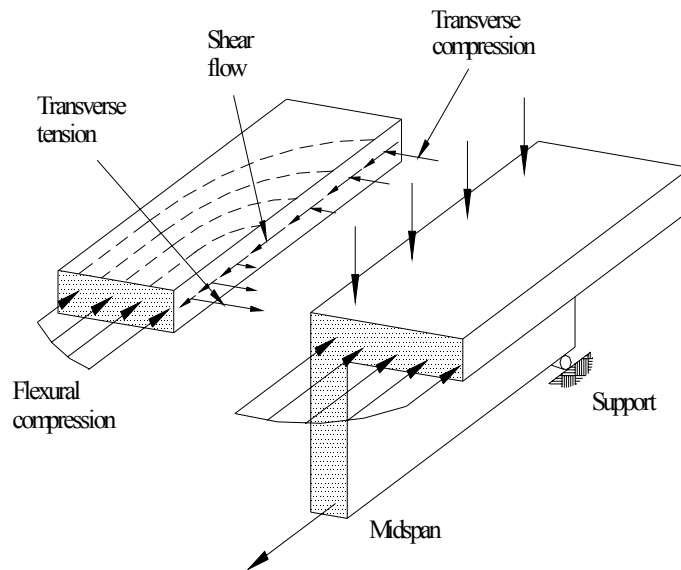


Figure 1.3 Forces on a T-beam

Figure 1.3 shows the forces acting on the flange of a simply supported T-beam. There are no compressive stresses in the flange at the supports because of zero moment value. However, when the midspan section is examined, the flexural compressive stresses will be observed to be distributed over the full width. This increment in flange from zero stress to full compressive stress causes horizontal shear stresses on the web-flange interface. As a result, there is what is called a “shear-lag” effect within the beam. This shear-lag effect causes higher stresses in the flange closest to the web and lower stresses in the flange away from the web as shown in Figure 1.3.

For a series of parallel beams, the flexural compressive stress distribution in the slab at a section of maximum positive moment is shown in Figure 1.4. The compressive stress reaches its maximum value over the web and decreases between the webs.

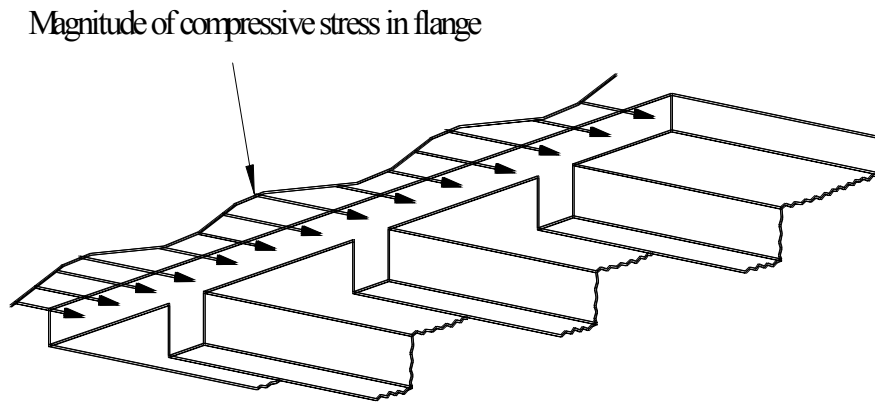


Figure 1.4 Distribution of maximum flexural compressive stresses  
(From MacGregor (2005))

Considering the actual stress distribution in a T-beam, the exact solution of T-beam problems is too time consuming for practical engineering calculations. Therefore, the familiar concept of effective width offers remarkable advantages in design. The actual stress distribution is replaced by a uniform linear stress distribution which provides the same compression. The width of this uniform stress block in the flange is called as “effective flange width”,  $b_e$ . The stress block for the effective width concept is illustrated in Figure 1.5.

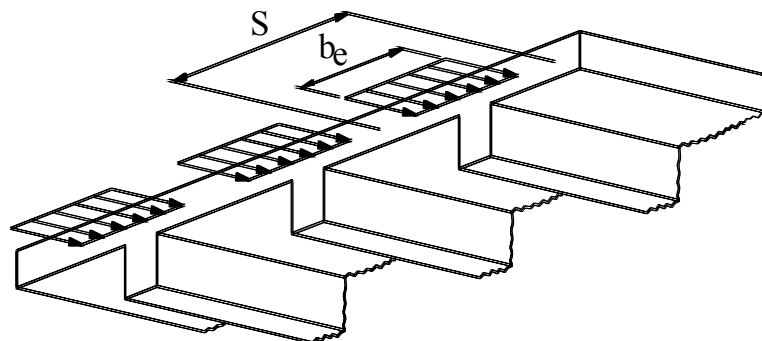


Figure 1.5 Uniform stress distribution and “effective flange width”

## **1.2. Survey of Previous Studies**

The effective width of wide beam flanges was investigated by Theodore von Karman which is discussed in Timoshenko's (1970) "Theory of Elasticity" book. The problem has been analyzed by minimum- energy principle using theory of elasticity.

In earlier attempts, folded plate theory or its equivalent was used to assess the effective width. The analysis were based either on stress criterion or deflection consideration. For example, Brendel (1964) used stress criterion in his analysis to determine the effective width. By contrast, the analysis done by Fraser and Hall (1973) was based on deflection considerations. A similar strategy was also used by Pecknold (1975) to assess the slab effective width for equivalent frame analysis.

Later on, Loo and Sutandi (1986) used a finite element analysis for simply supported T-beams utilizing solid elements. From the resulting data on the effective width, they derived empirical design formulas using statistical means.

In a quite recent investigation, a similar approach has been used by Utku and Aygar (2002) who extended this to derive design formulas for the effective flange width of continuous T-beams using a three-dimensional finite element analysis.

## **1.3. Scope of Thesis**

In the present study, a new formulation is proposed for the evaluation of the effective flange width formulas for continuous T-beams. The analysis is

based on a deflection criterion. The codes of various countries have certain limitations and may be considered as approximate, since they are expressed only in terms of span length or flange and web thicknesses, but they ignore the loading conditions and other significant parameters. In this study, a three-dimensional finite element analysis is carried out on continuous T-beams. The beam spacing, span length, overall depth, web thickness and flange thickness are considered as independent variables in the analysis. The derivation of the effective flange width employs usual elastic beam theory and the displacement results of the finite element solution. The effective flange width for each beam is calculated analytically and design formulas are derived for the corresponding two different loading conditions by using nonlinear regression analysis. The proposed formulas are compared with the available code recommendations and presented in graphical format.

The study is organized as follows. In Chapter 1, an introduction to the thesis and a limited survey of previous work done on the subject is presented. In Chapter 2 the concept of effective flange width and theoretical basis for determination of effective width are given. TS-500, Eurocode 2, ACI and BS-8110 code recommendations are also presented in this chapter. The proposed formulation is then presented in Chapter 3. Analytic solutions are given for deflection, shear and moments of continuous beams for two different load cases. Finite element analysis for two different loading conditions is also given in Chapter 3 and Chapter 4. In Chapter 5, empirical design formulas are derived using nonlinear regression analysis. The new formulation is compared with the code recommendations. Finally, Chapter 6 discusses the results and includes conclusions and recommendations.

## CHAPTER 2

### EFFECTIVE FLANGE WIDTH AND CODE RECOMMENDATIONS

#### 2.1. Concept of Effective Flange Width

Considering the number of factors affecting the actual stress distribution in a T-beam such as the type of loading (uniform, concentrated), the type of supports, the spacing of the beams, the dimensions of the cross section, the T-beam design is a rather complex problem. Therefore the familiar concept of “effective flange width” has been accepted by the profession for many decades. Effective flange width offers remarkable advantages; it enables the designer to apply simple bending formulas of rectangular sections to T-beams. Under the assumption of a straight neutral axis and the proportionality of all stresses to the distance from this axis, the effective width of the flanges can be defined. Simple bending formulas can now be used to furnish the actual extreme fiber stress  $\sigma_{y_{\max}}$  of the concrete at the top of the section and the actual total compressive force. The stress block for effective width concept is indicated in Figure 2.1.

Because of simplicity, its use is still being recommended in all known codes of practice. Three of them are going to be presented in the following sections. The code equations can only be very approximate as they are

expressed merely in terms of span length or flange and web thicknesses, but they ignore other significant variables mentioned above.

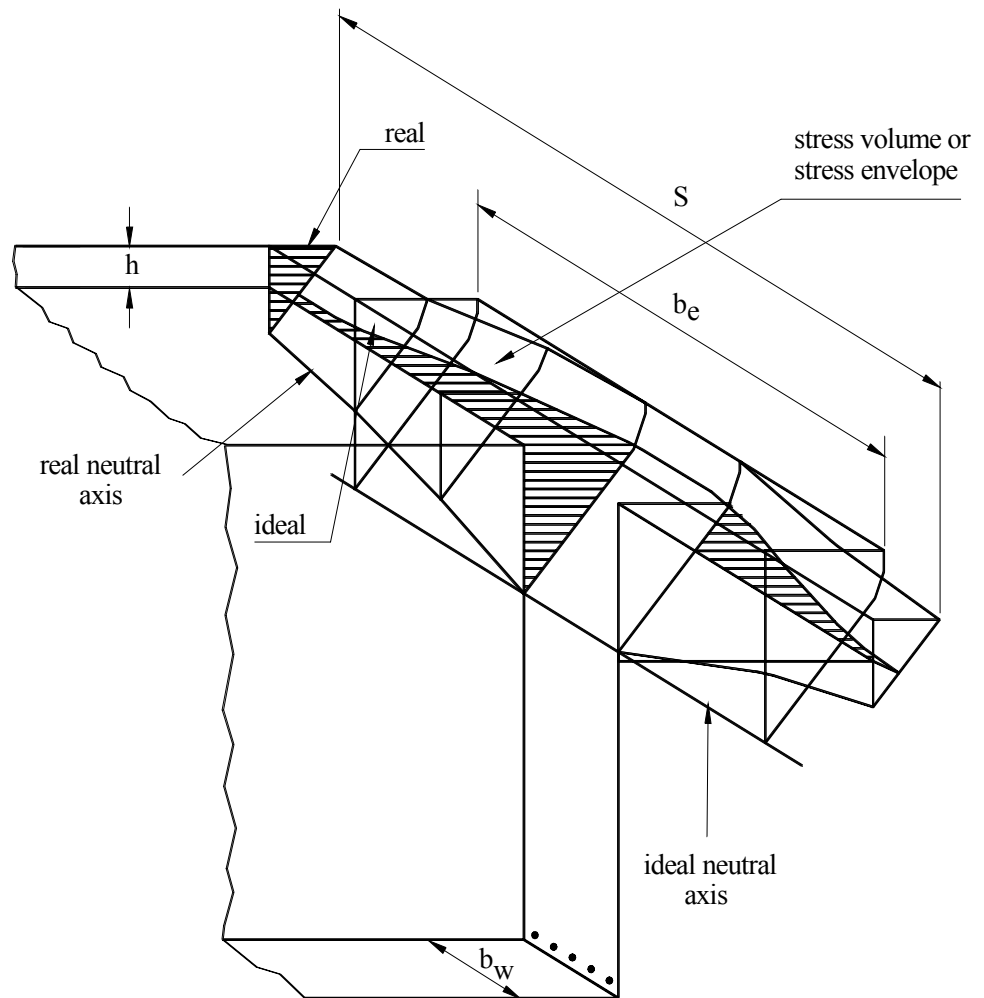


Figure 2.1 Compressive stress block of T-section (From Brendel (1964))

## **2.2 Code Recommendations**

### **2.2.1. ACI Building Code**

#### **T-Beam construction:**

This section contains provisions identical to those of previous ACI Building Codes for limiting dimensions related to stiffness and flexural calculations. Special provisions related to T-beams and other flanged members are stated in part 11.6.1. of the code with regard to torsion.

- In T-beam construction, the flange and web shall be built integrally or otherwise effectively bonded together.
- Width of slab effective as a T-beam flange shall not exceed one-quarter of the span length of the beam, and the effective overhanging flange width on each side of the web shall not exceed:
  - (a) eight times the slab thickness, and
  - (b) one-half the clear distance to the next web.
- For beams with a slab on one side only, the effective overhanging flange width shall not exceed:
  - (a) one-twelfth the span length of the beam,
  - (b) six times the slab thickness, and
  - (c) one-half the clear distance to the next web.
- Isolated beams, in which the T-shape is used to provide a flange for additional compression area, shall have a flange thickness not less than one-half the width of web and an effective flange width not more than four times the width of web.
- Where primary flexural reinforcement in a slab that is considered as a T-beam flange (excluding joist construction) is parallel to the beam,

reinforcement perpendicular to the beam shall be provided in the top of the slab in accordance with the following:

- Transverse reinforcement shall be designed to carry the factored load on the overhanging slab width assumed to act as cantilever.
- For isolated beams, the full width of overhanging flange shall be considered. For other T-beams, only the effective overhanging slab width needs to be considered.
- Transverse reinforcement shall be spaced not farther apart than five times the slab thickness, or 18 in (45.7 cm).

### 2.2.2. Eurocode

#### Effective Flange Width:

- The effective flange width of a flange,  $b_{eff}$ , should be based on the distance,  $l_0$ , between points of zero moments as shown in Figure 2.2 and defined in Figure 2.3.

$$b_{eff} = b_w + b_{eff,1} + b_{eff,2} \quad (2.1)$$

where

$$b_{eff,1} = (0.2b_1 + 0.1l_0) \text{ but } \leq 0.2l_0 \text{ and } \leq b_1 \quad (2.2)$$

$b_{eff,2}$  = to be calculated in a similar manner to  $b_{eff,1}$  but  $b_2$  should be substituted for  $b_1$  in the above

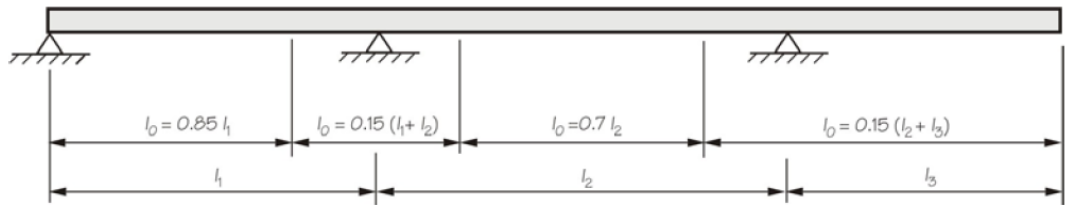


Figure 2.2 Elevation showing definition of  $l_0$  for calculation of flange width

- The distance  $l_0$  between points of zero moment may be obtained from Figure 2.2 for typical cases.

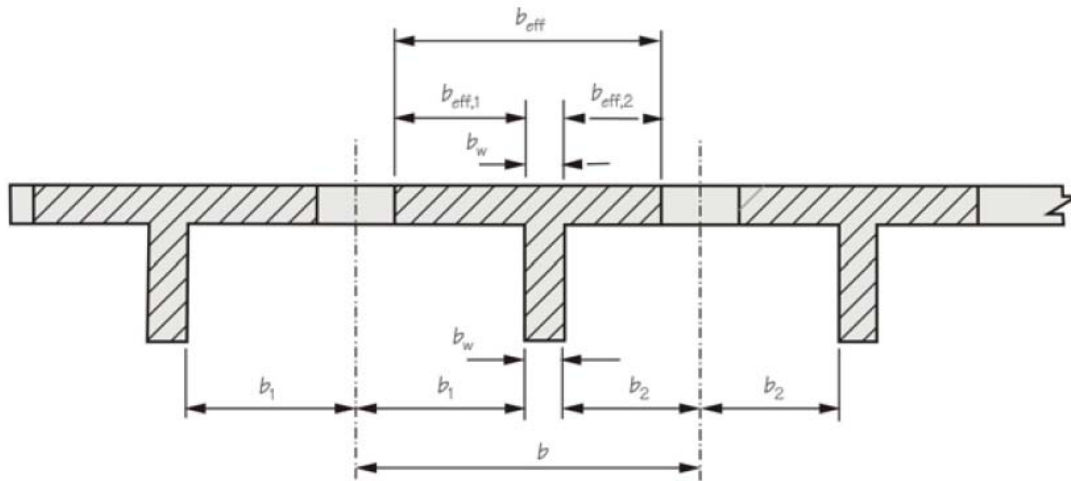


Figure 2.3 Section showing effective flange width parameters

### 2.2.3. TS 500

In dimensioning the flanged sections, the flange width, which is required to calculate the necessary moment of inertia for structural analysis and in finding the deflections must be calculated by using the equations below, referring to Figure 2.4.

In symmetrical sections:

$$b = b_w + \frac{1}{5} l_p \quad (2.3)$$

In nonsymmetrical sections:

$$b = b_w + \frac{1}{10} l_p \quad (2.4)$$

On the other hand, the overhanging flange width on each side of the web shall not exceed six times the flange thickness and one-half the clear distance to the next web ( $\leq 6h_f$  or  $1/2a_n$ ). In equations (2.3) and (2.4),  $l_p$  is the distance between the points of zero moments and  $l$  is the span length ( $l_p = \alpha l$ ). For analysis, when a great accuracy is not required, the following values for  $\alpha$  can be used.

Table 2.1 Values for  $\alpha$

Simply supported beams	$\alpha = 1.0$
Continuous beams (edge span)	$\alpha = 0.8$
Continuous beams (middle span)	$\alpha = 0.6$
Cantilever beams	$\alpha = 1.5$

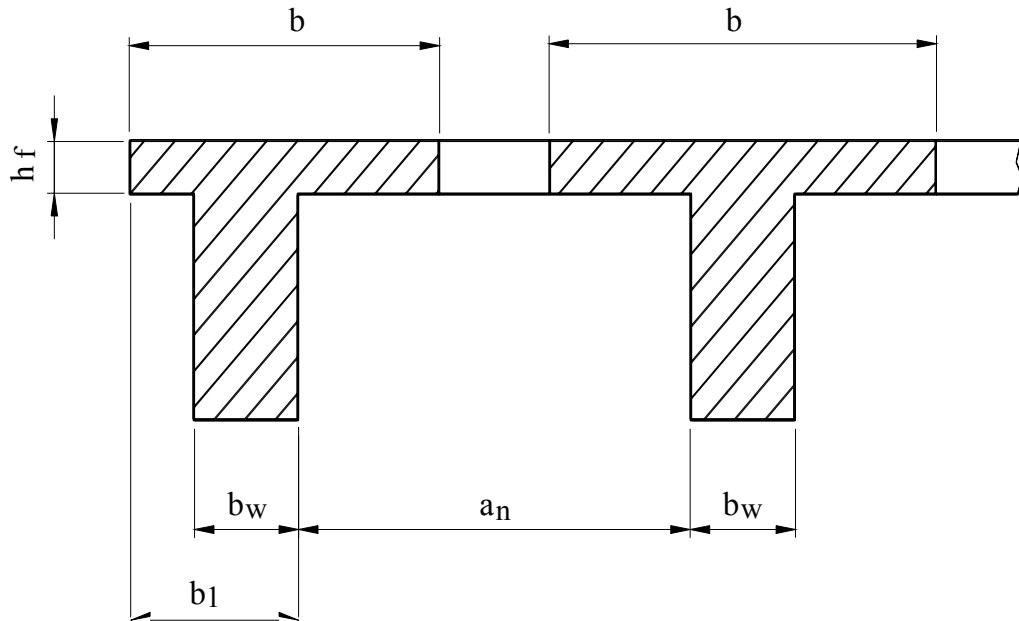


Figure 2.4 Definition of dimensions in T-beams

#### 2.2.4. British Standards BS-8110

In the absence of any more accurate determination effective flange width should be taken as:

- a) for T-beams: web width  $+l_z/5$  or actual flange width if less;
- b) for L-beams: web width  $+l_z/10$  or actual flange width if less;

where

$l_z$  is the distance between points of zero moment (which, for a continuous beam, may be taken as 0.7 times the effective span).

## **CHAPTER 3**

### **FORMULATION OF THE PROBLEM**

#### **3.1 Effective Flange Width Based on Deflection Criterion**

In this study, the effective flange width of T-beams is investigated based on displacement criterion. The derivation of effective width employs usual elastic beam theory and matching the equation of the elastic curve with the beam deflections obtained from finite element analysis.

As mentioned in Chapter 1, two types of loading are considered. As the first case, the beam is exposed to point loads at midspan. Uniformly distributed load on the flange is the second load case. Analytical (Closed Form) solutions for both cases are given in the following sections.

#### **3.2 Point Load at Midspan**

In this type of loading, point loads are applied at midpoint of each span as shown in Figure 3.1.

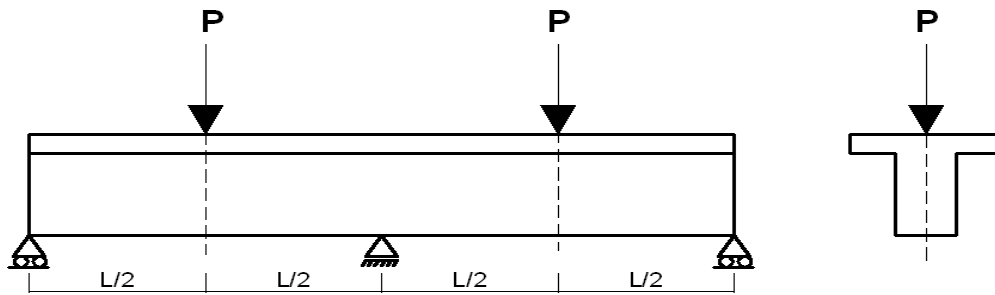


Figure 3.1 Load at midspan

The differential equation of the elastic curve of the beam is obtained by direct integration. Due to symmetry, only the left span is considered in the calculations. For the beam considered, the bending moment equations for the intervals  $0 \leq x \leq L/2$  and  $L/2 \leq x \leq L$  are substituted into the differential equation of the elastic curve. The two differential equations are integrated twice to obtain the equations of the elastic curve for each interval. These equations contain four constants of integration which are evaluated by using the boundary conditions

$$v_1(0) = v_2(L) = 0$$

and the continuity conditions

$$\frac{dv_1(L/2)}{dx} = \frac{dv_2(L/2)}{dx}, \quad v_1(L/2) = v_2(L/2)$$

where  $v_1$  is the deflection for  $0 \leq x \leq L/2$  and  $v_2$  is the deflection for  $L/2 \leq x \leq L$ . Shear, moment, and deflection diagrams for this beam are shown in Figure 3.2.

The elastic curve for interval  $0 \leq x \leq L/2$  becomes

$$v(x) = \frac{P}{96EI} (5x^3 - 3L^2x) \quad (3.1a)$$

For  $L/2 \leq x \leq L$ :

$$v(x) = \frac{P}{96EI} \left\{ 5x^3 - 16\left(x - \frac{L}{2}\right)^3 - 3L^2x \right\} \quad (3.1b)$$

The point of maximum deflection is at  $x = L / \sqrt{5}$ , which follows from setting the expression for the slope equal to zero. The deflection at this point is

$$|v|_{\max} = \frac{PL^3}{48\sqrt{5}EI} \quad (3.2)$$

For the point load case, the maximum flexural stress occurs at the loading points. The deflection at applied load  $P$ , which will be used later for the effective width calculations, is

$$v(L/2) = -\frac{7PL^3}{768EI} \quad (3.3)$$

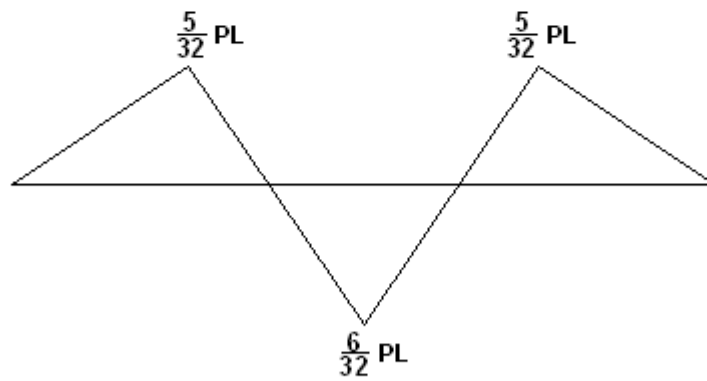
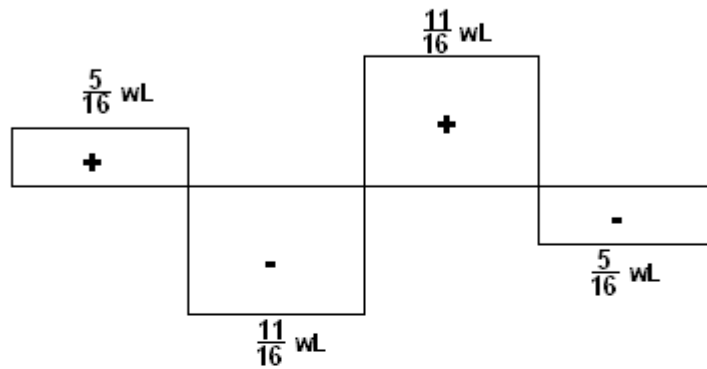
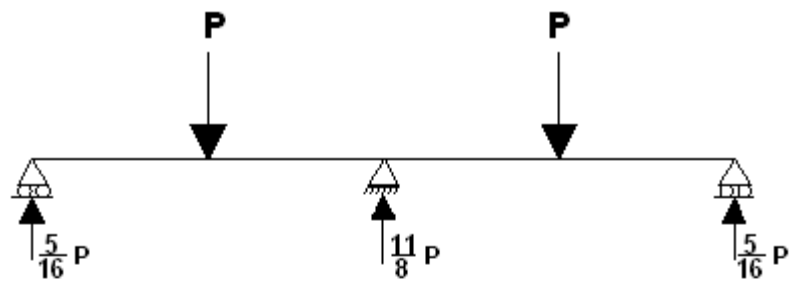


Figure 3.2 Shear, moment, and deflection diagrams for load at midspan

### 3.3 Uniformly Distributed Load on Flange

As a second load case, the uniformly loaded continuous beam shown in Figure 3.3 is considered. The beam supports a uniform load of  $w$  per unit length which results from a uniform pressure  $p$  applied on the flange.

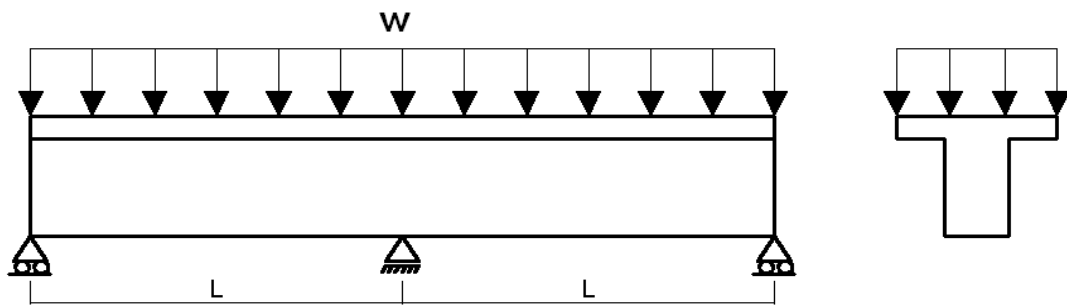


Figure 3.3 Uniformly distributed load

The length of each span is  $L$ , and because of symmetry, the solution is obtained by considering the deflection for either span. Following similar steps as in the point load case, shear, moment, and deflection diagrams appear as shown in Figure 3.4.

The elastic curve for interval  $0 \leq x \leq L$  becomes

$$v(x) = -\frac{wx}{48EI}(L^3 - 3Lx^2 + 2x^3) \quad (3.4)$$

The largest deflection occurs at  $x = 0.422 L$ , which follows from setting the expression for the slope equal to zero. The deflection at this point is

$$|v|_{\max} = -5.416 \times 10^{-3} \frac{wL^4}{EI} \quad (3.5)$$

For the uniformly distributed load, the maximum compressive stress occurs at  $x = 3L / 8$  from the left support. The deflection at  $x = 3L / 8$ , which will be used later for the effective width calculations, is

$$v(3L/8) = -5.3406 \times 10^{-3} \frac{wL^4}{EI} \quad (3.6)$$

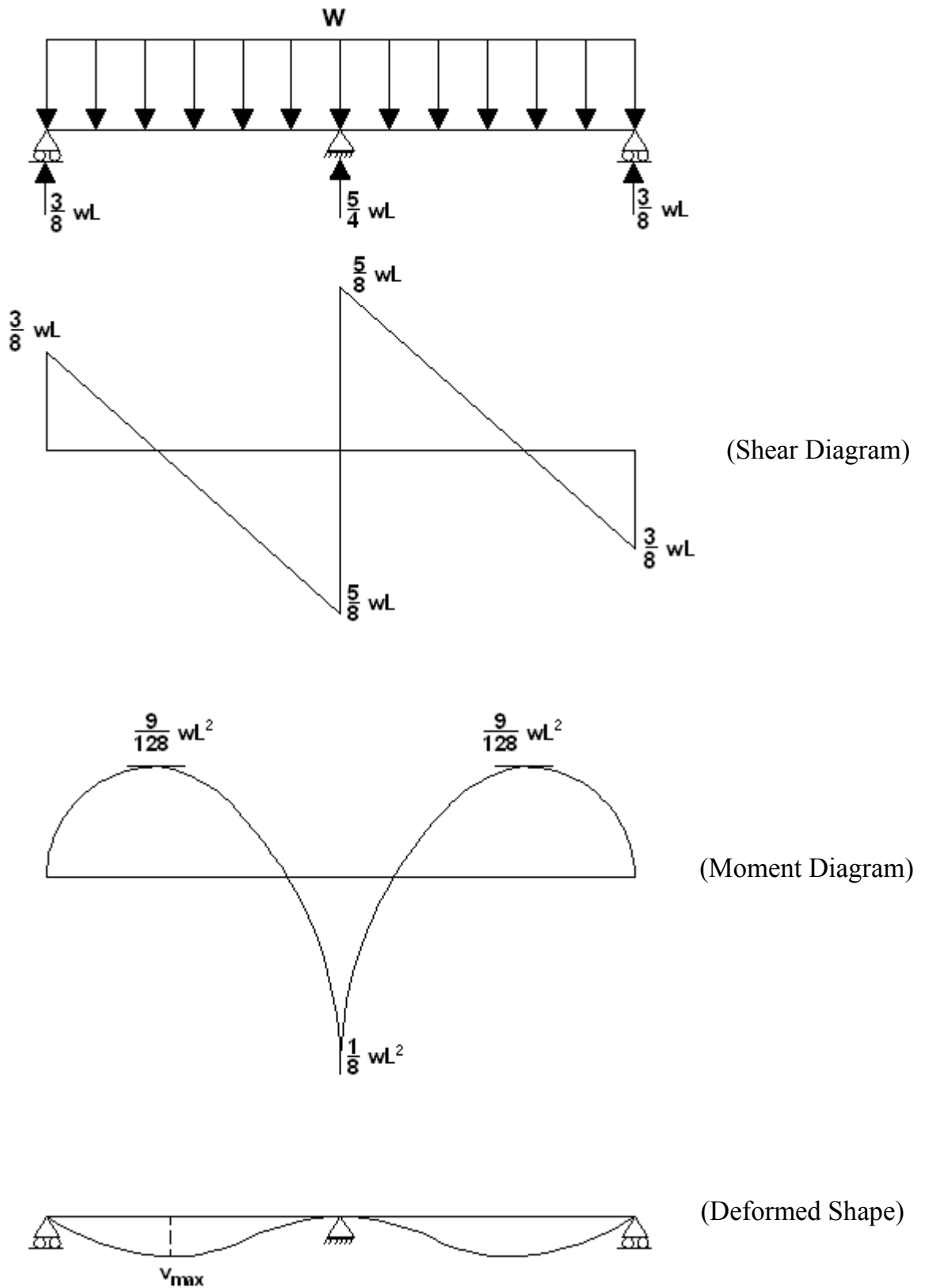


Figure 3.4 Shear, moment, and deflection diagrams for uniform loading

### 3.4 Transformed T-Section

An interior beam of a beam-and-slab floor system develops positive moments at midspan and negative moments over the support. At midspan, the compression zone is in the flange. For the computation of effective width two cases are possible:

- 1) the neutral axis may shift down into the web, giving a T-shaped compression zone, and
- 2) the neutral axis is in the flange and hence, the compression zone is rectangular.

For the first case where the neutral axis passes through the web (see Figure 3.5), the calculation is as follows.

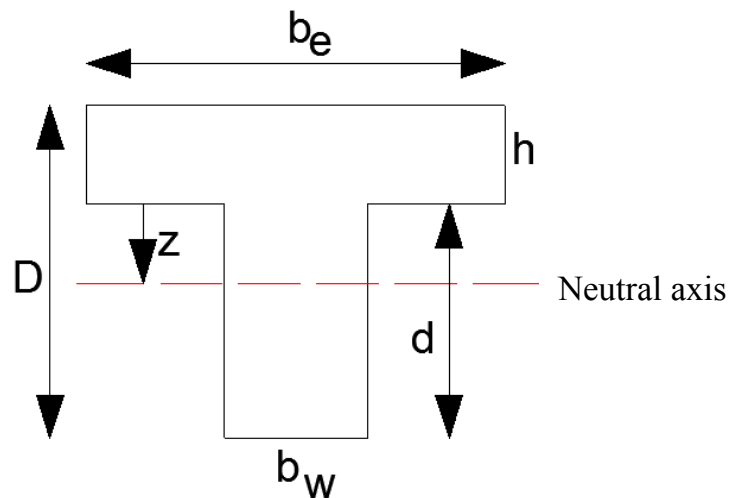


Figure 3.5 Neutral axis passing through the web

The beam cross-section is examined in three parts. The first part is a rectangular area defined by the flange width  $b_e$  and flange thickness  $h$ . The second part is that portion of the web with height  $x$  and web thickness  $b_w$  as shown in Figure 3.6b. Finally; the third part consists of the web below the

neutral axis as illustrated in Figure 3.6c. Area moments of these three parts are calculated separately and place of centerline is determined.

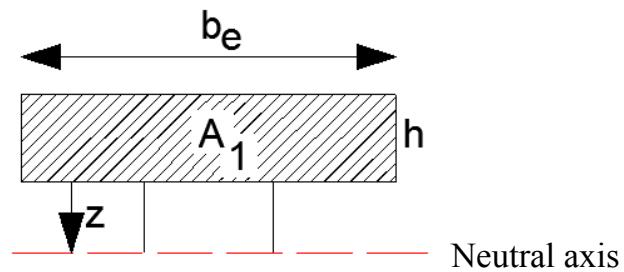


Figure 3.6a Part  $A_1$  of the cross-section

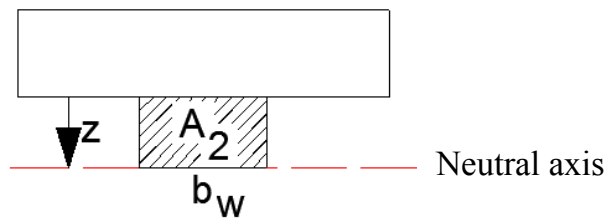


Figure 3.6b Part  $A_2$  of the cross-section

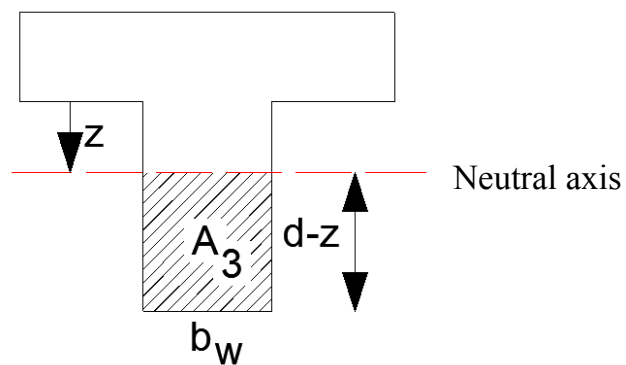


Figure 3.6c Part  $A_3$  of the cross-section

The area of each component part and the moments of the component areas with respect to the neutral axis are then computed.

$$\begin{aligned}
A_1 &= h \times b_e & M_{A1} &= h \times b_e \times \left(\frac{h}{2} + z\right) \\
A_2 &= b_w \times z & M_{A2} &= b_w \times z \times \left(\frac{z}{2}\right) \\
A_3 &= b_w \times (d - z) & M_{A3} &= b_w \times \frac{(d - z)^2}{2}
\end{aligned}$$

For the third part (D-h) term is replaced by  $d$  in order to simplify the expressions. Equating the first moment of the area on one side of the neutral axis to the first moment of the area on the other side,

$$M_{A1} + M_{A2} = M_{A3} \quad (3.7)$$

$$h \times b_e \times \left(\frac{h}{2} + z\right) + b_w \times \left(\frac{z^2}{2}\right) = b_w \times \frac{(d - z)^2}{2}$$

It has to be noted that  $z$  in the above formula represents the distance between the neutral axis and the bottom of the flange. By solving Eq.(3.7) with flange thickness  $h$  equal to 12 cm, the distance  $z$  is obtained as

$$z = \frac{\frac{b_w \times d^2}{2} - 72 \times b_e}{12 \times b_e + b_w \times d} \quad (3.8)$$

It is observed that the distance  $z$  given by Eq. (3.8) depends on the effective width  $b_e$  which is an unknown quantity at the moment. Finally, the moment of inertia for the transformed T-section can be written in terms of  $z$  and  $b_e$  as

$$I_{beam} = h \times b_e \times \left(z^2 + hz + \frac{h^2}{3}\right) + \frac{b_w}{3} \times (z^3 + (d - z)^3) \quad (3.9)$$

For the second case where the neutral axis is passing through the flange (see Figure 3.7), the steps for the calculation of the neutral axis and the moment of inertia are same as the first case where centerline was within the web.

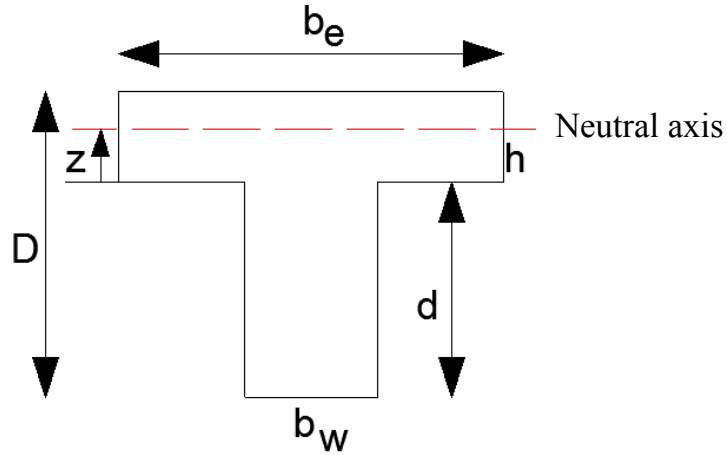


Figure 3.7 Neutral axis passing through the flange

After the necessary calculations, the following expressions are obtained for the position of the neutral axis, and the moment of inertia.

$$z = \frac{72 \times b_e - \frac{b_w \times d^2}{2}}{12 \times b_e + b_w \times d} \quad (3.10)$$

$$I_{beam} = \frac{b_e}{3} \times ((h - z)^3 + z^3) + b_w \times d \times (dz + z^2 + \frac{d^2}{3}) \quad (3.11)$$

The effective flange width  $b_e$  is calculated by equating the above expression for the moment of inertia to the numerical value computed from finite element displacement results as explained in Section 4.4 on “Numerical Studies”.

## CHAPTER 4

### FINITE ELEMENT ANALYSIS

#### 4.1 The Solid Element

The finite element method is the most appropriate numerical tool for the displacement and stress analysis for structural systems. In the finite element models adopted in this study, the solid elements are used to model the beam-and-slab floor system. The software SAP2000 v.11.0, which is one of the widely used finite element analysis programs, is used for the three-dimensional modeling and displacement analysis. A  $2 \times 2 \times 2$  numerical integration scheme is used for the solid element. Stresses in the element local coordinate system are evaluated at the integration points and extrapolated to the joints of the element. Six stress components are calculated as nodal average stresses, the three normal stresses and the three shear stresses.

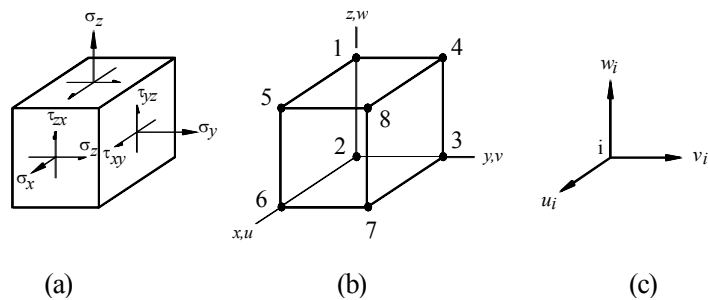


Figure 4.1 (a) Three-dimensional state of stress. (b) Eight-node solid element. (c) Degrees of freedom at a typical node ( $i= 1, 2... 8$ )

The eight-node element shown in Figure 4.1 has eight nodes located at the corners and has three translational degrees of freedom at each node. In terms of generalized coordinates  $\beta_i$ , the displacement field can be written as

$$\begin{aligned} u &= \beta_1 + \beta_2 x + \beta_3 y + \beta_4 z + \beta_5 xy + \beta_6 yz + \beta_7 zx + \beta_8 xyz \\ v &= \beta_9 + \beta_{10} x + \beta_{11} y + \beta_{12} z + \beta_{13} xy + \beta_{14} yz + \beta_{15} zx + \beta_{16} xyz \\ w &= \beta_{17} + \beta_{18} x + \beta_{19} y + \beta_{20} z + \beta_{21} xy + \beta_{22} yz + \beta_{23} zx + \beta_{24} xyz \end{aligned} \quad (4.1)$$

The eight-node element can be of arbitrary shape when it is formulated as an isoparametric element (Cook et. al. 1989). The coordinates used are shown in Figure 4.2.

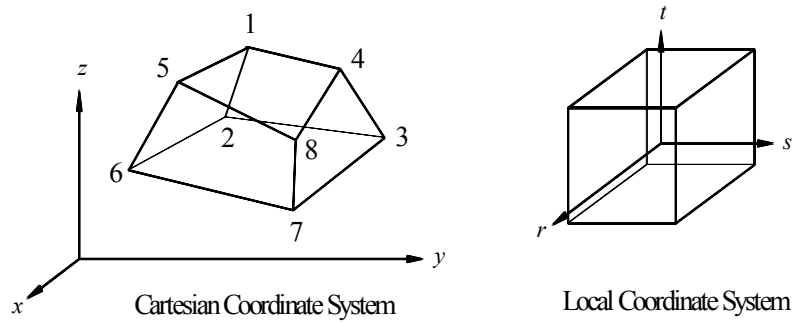


Figure 4.2 Eight-node isoparametric solid element

The displacement expressions can then be written as

$$u = \sum N_i u_i \quad v = \sum N_i v_i \quad w = \sum N_i w_i \quad (4.2)$$

where the index  $i$  runs from 1 to 8 in each summation. The shape functions defining the geometry and variation of displacements are given by,

$$N_i = \frac{1}{8} (1 + r r_i) (1 + s s_i) (1 + t t_i) \quad i=1, 2, \dots, 8$$

where  $r$ ,  $s$  and  $t$  are local (natural) coordinates and  $r_i$ ,  $s_i$ ,  $t_i$ , are the values of local coordinates for node  $i$ .

## 4.2 Parameters Influencing the Effective Flange Width

It is known from the available literature on T-beams that the effective width  $b_e$  is affected by sectional dimensions and by the beam span  $L$  for both uniformly distributed and concentrated load. In the following finite element analysis, the effect of various parameters on the effective flange width is studied. These parameters include the beam spacing  $S$ , beam span length  $L$ , total depth of the beam  $D$ , web thickness  $b_w$ , and flange thickness  $h$ , as shown in Figure 4.3.

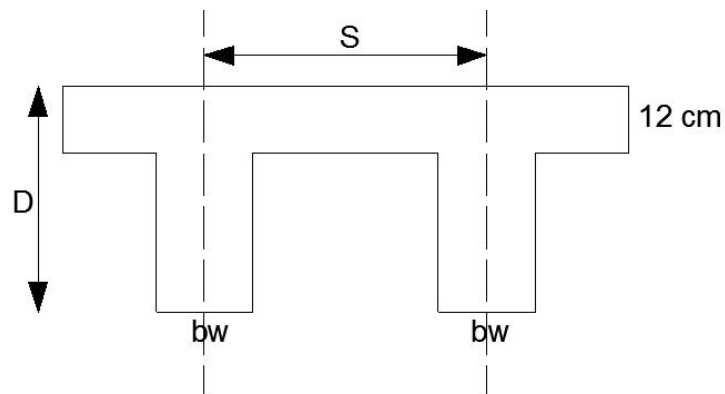


Figure 4.3 Dimensions of a T-beam

These parameters are independent variables that influence the effective flange width  $b_e$ . In addition to the above parameters, the effect of loading type is also considered as another parameter for the investigation of effective flange width. Uniformly distributed load and concentrated load at midspan are the two loading types applied separately on the three dimensional finite element models.

In order to investigate the dependency of effective flange width on these parameters, they are varied in a systematic way using a combination of the ratios of the beam parameters. Specifically, the ratios of  $S/L$ ,  $L/D$ ,  $b_w/D$  and  $h/D$  are defined in groups of three to provide data for deriving the design formulas. In finite element analysis, the flange thickness  $h$  is considered as constant for all T-beams. The flange thickness is assumed to be 120 mm, and the dimensional parameters are varied as shown in Table 4.1.

Table 4.1 Dimensionless parameters

S/L	0.20	0.25	0.30
L/D	10	15	20
$b_w/D$	0.65	0.70	0.75
h/D	0.20	0.30	0.40

These require 81 T-beams for each of the three loading conditions defined in Figure 3.1 and Figure 3.3. This results in a total number of 162 finite element analyses.

### 4.3 Finite Element Model

This study is performed for a two-span continuous T-beam. Due to double symmetry only a quarter of the beam over a span length  $L$  is modeled by using solid elements. Boundary conditions are specified taking into consideration symmetry and the simple-support conditions. The symmetry boundary conditions are applied on two planes. The vertical  $yz$ -plane is a plane of symmetry. For nodes of the finite element mesh on this plane, the displacement degree of freedom in  $x$ -direction is fixed. Similarly, the transverse  $xz$ -plane at the middle support is another plane of symmetry. For

all nodes on this plane, on the other hand, the displacement degree of freedom in  $y$ -direction is fixed.

The finite element beam model is meshed into nearly equal sized elements which have aspect ratios near unity. This requirement results in a finite element mesh in which the beam is divided into 64 equal segments along the beam span. On a transverse section, the flange is divided into 3 segments in the vertical direction. The symmetrical half of the web below the flange is divided into 8 equal segments in the vertical dimension. For each transverse section, there are 27 elements in the flange and 24 elements in the web. These result in a total of 3264 elements and 4680 nodal points.

In the finite element analysis of the T-beam, the modulus of elasticity for concrete is taken as 30 GPa. The Poisson's ratio is assumed to be 0.2 and the total load intensity is taken as 20 kN/m<sup>2</sup>. The self weight of the beam is neglected in the analysis. The distributed load is applied as force per unit area on the flange for the uniformly distributed load case. For the point load case, concentrated loads are applied at the appropriate nodes. A longitudinal view of the model is illustrated in Figure 4.4. A cross section of the model and a typical three dimensional finite element mesh used for the analysis are shown in Figure 4.5a and 4.5b respectively. The stress distribution and the deformed shapes for typical cases are also given in Figures 4.6 through 4.9.

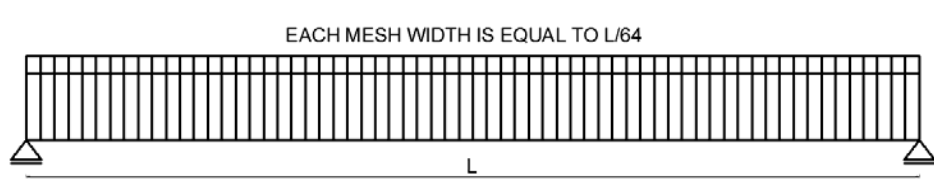


Figure 4.4 Longitudinal view of the finite element model

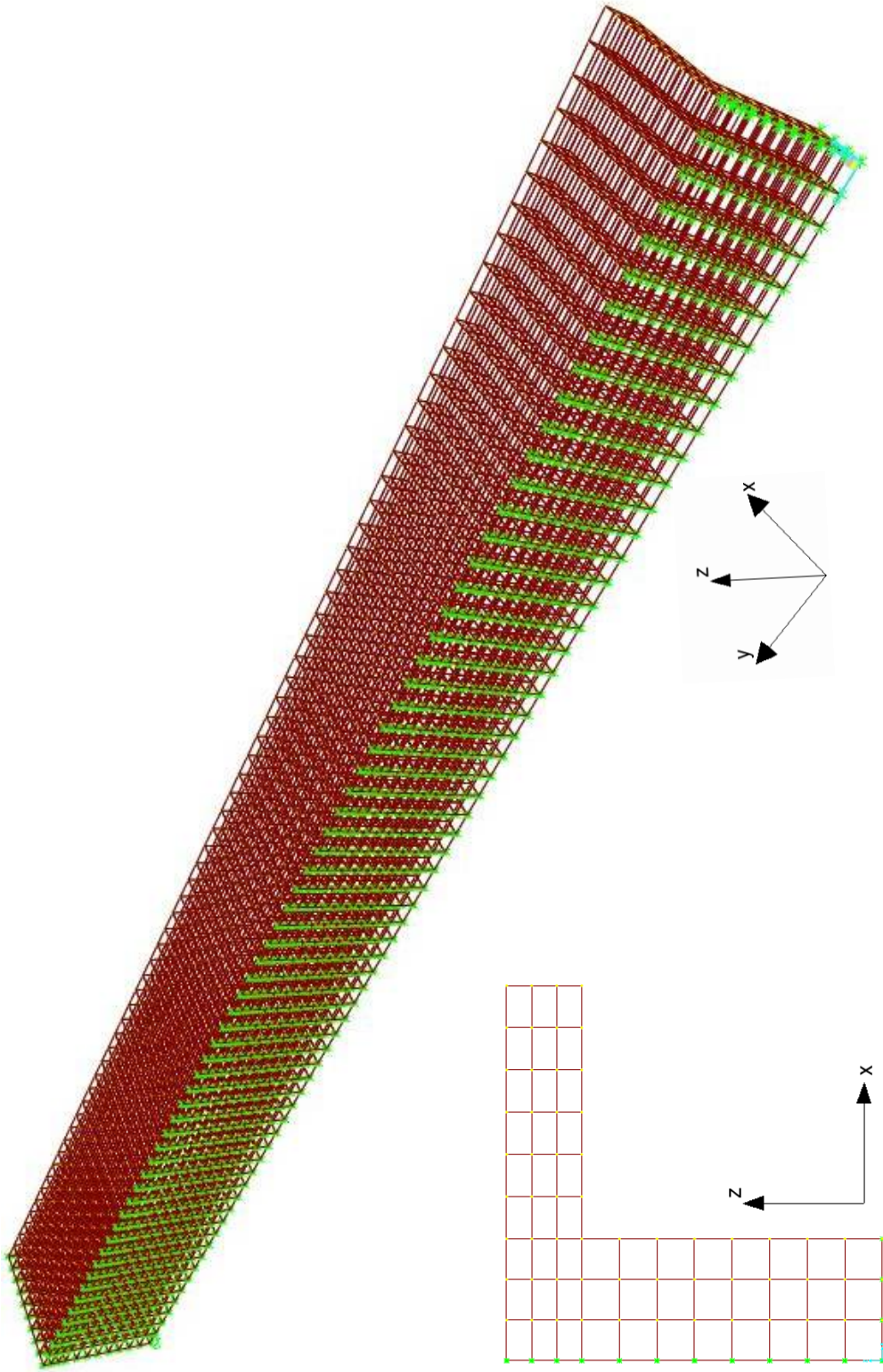


Figure 4.5a Cross section of the finite element model

Figure 4.5b Three dimensional finite element model

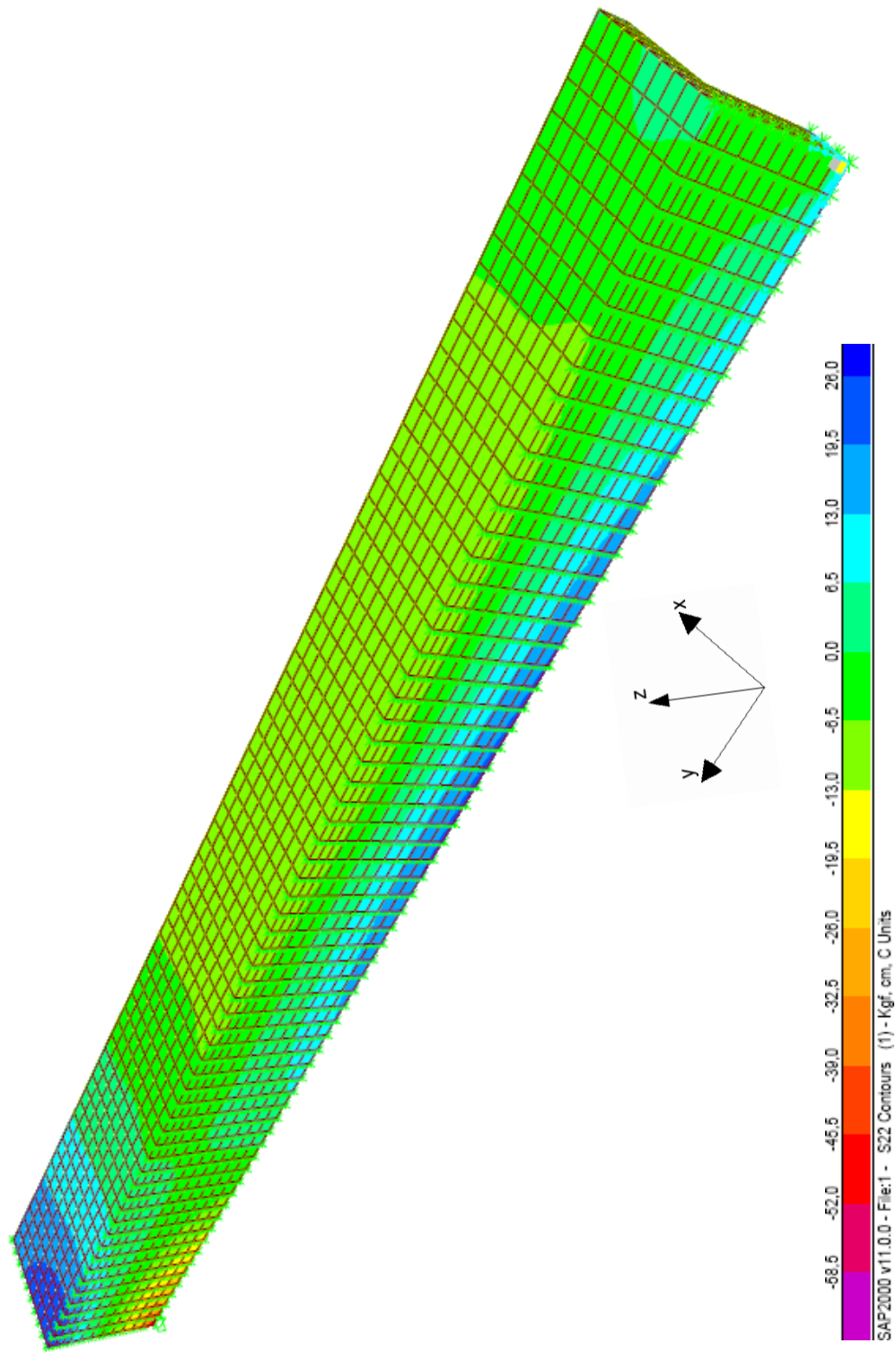


Figure 4.6 Flexural stress distribution for uniform loading

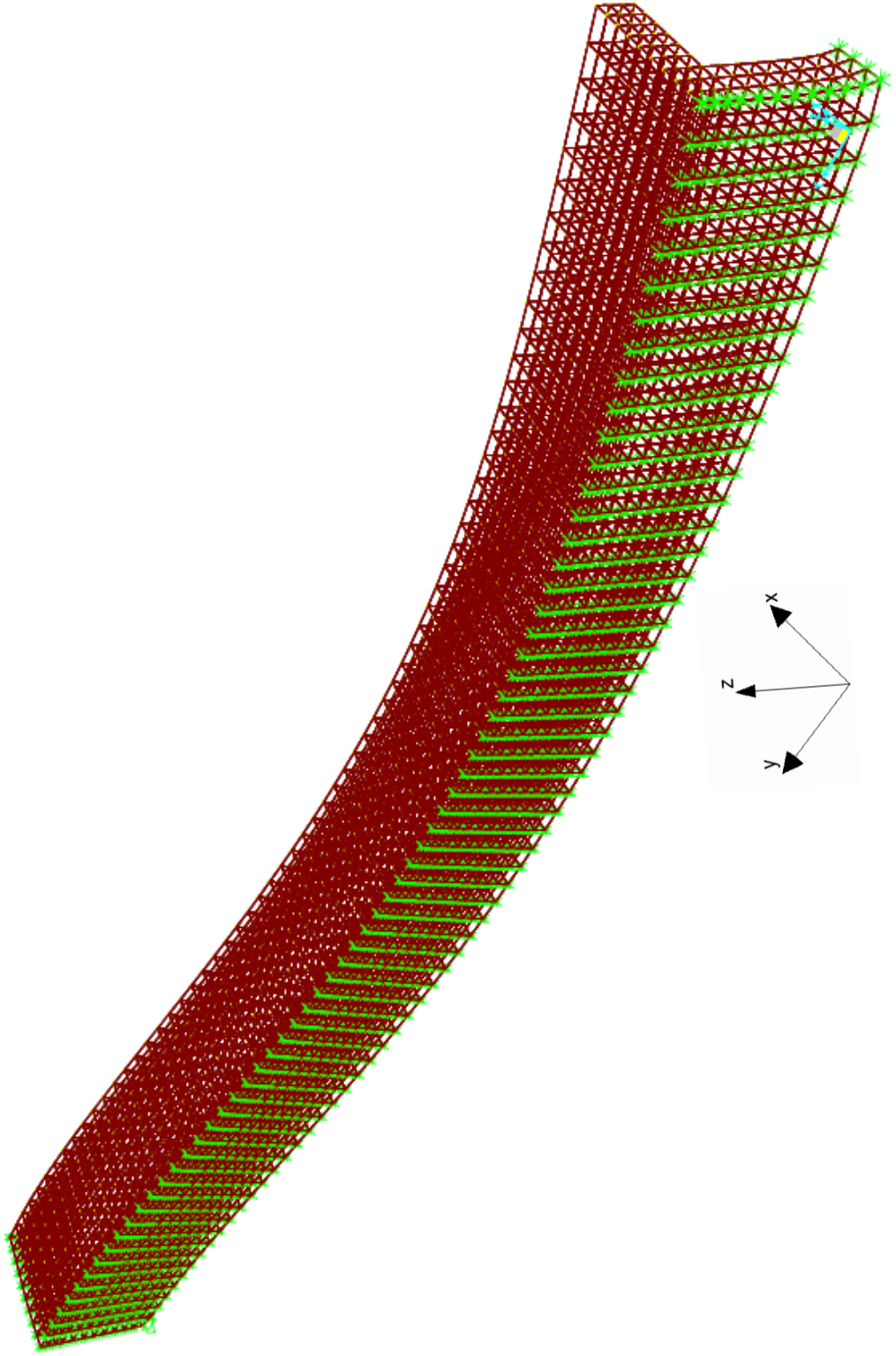


Figure 4.7 Deformed shape under uniform loading

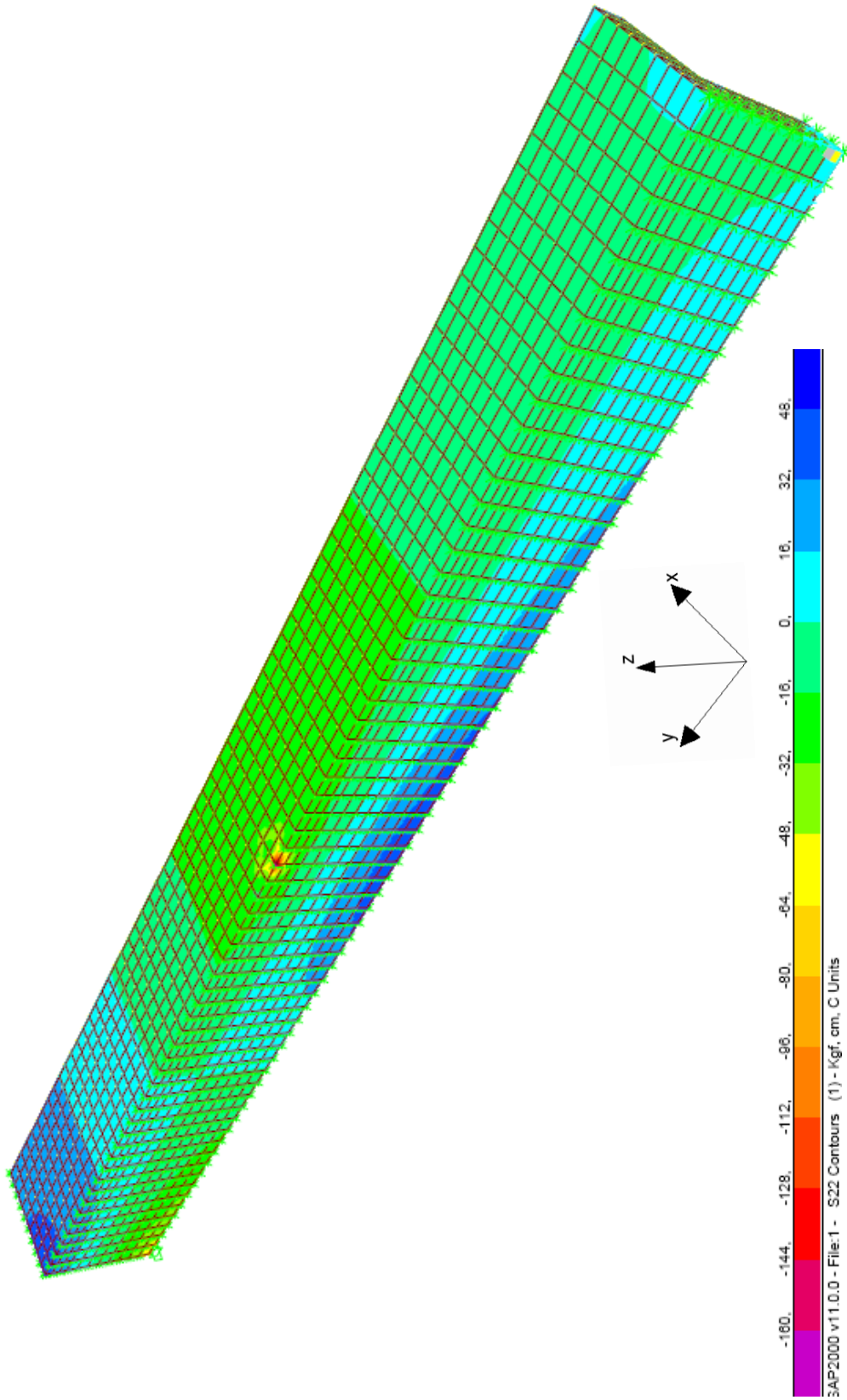


Figure 4.8 Flexural stress distribution for loading at midspan

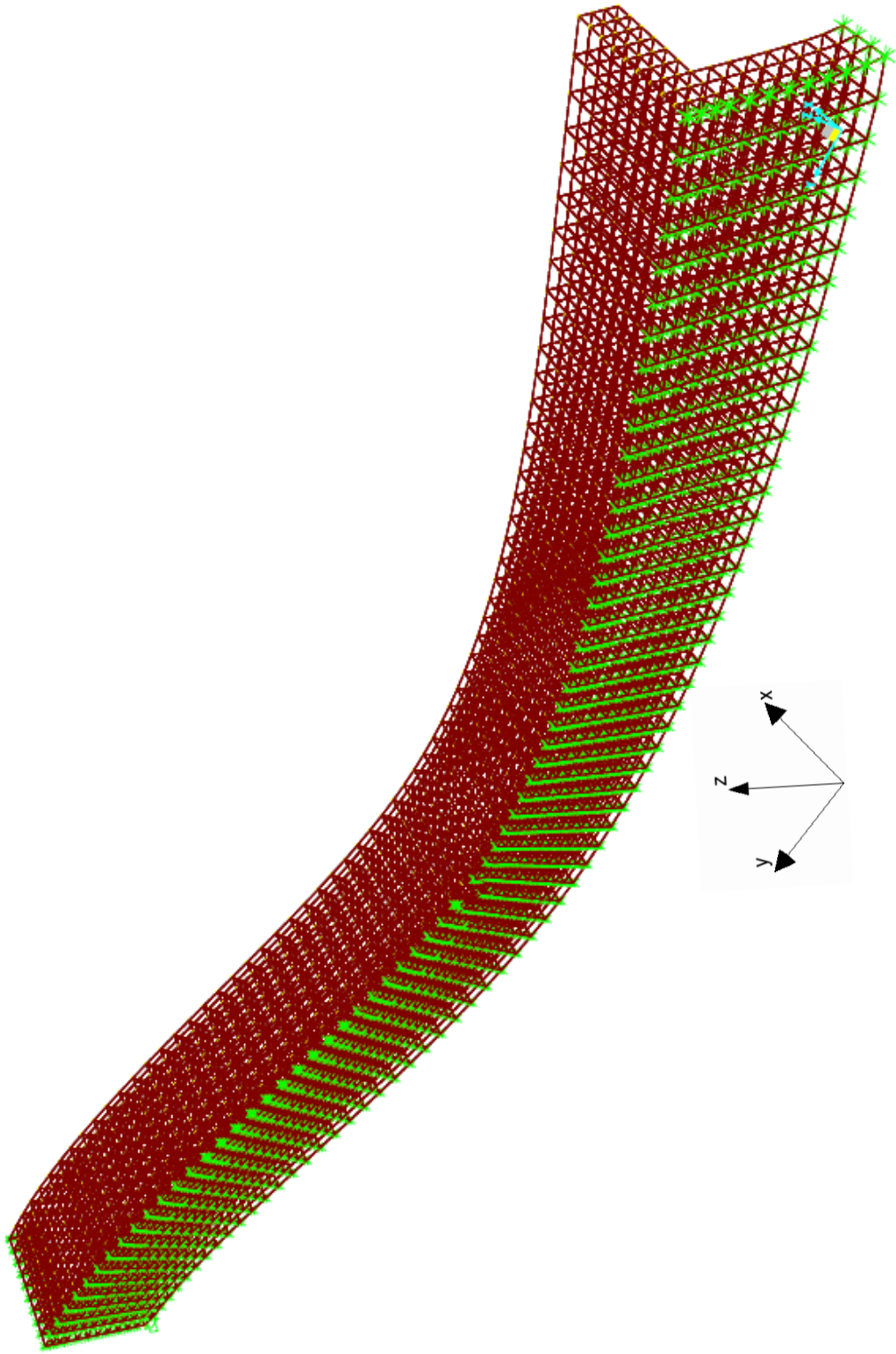


Figure 4.9 Deformed shape under loading at midspan

#### 4.4 Numerical Studies

In the concept of effective width, the actual distribution of the flexural compressive stresses in the flange is replaced by a uniform distribution to produce the same total compression. Since, almost the full flange width is stressed in compression at a section of maximum positive moment; the reduction to effective width is also done at this section.

Motivated by the above strategy, the beam deflections at the section of maximum positive moment are equated to the displacements obtained from a three-dimensional finite element analysis of the beam-and-slab floor system. For point load cases, the maximum positive moment and hence the maximum compressive stress occurs at the loading points. By using Eq. (3.3), the equivalence expression for beam deflections at  $x = L / 2$  is

$$v_{FE}(L/2) = v(L/2) = -\frac{7PL^3}{768EI} \quad (4.3)$$

Hence, the moment of inertia of the T-section is

$$I_T = -\frac{7PL^3}{768 E v_{FE}(L/2)} \quad (4.4)$$

For the uniformly distributed load, on the other hand, the maximum compressive stress occurs at  $x = 3L / 8$  from the left support. Then, equating the finite element deflections to beam deflections given by Eq. (3.6),

$$v_{FE}(3L/8) = v(3L/8) = -5.3406 \times 10^{-3} \frac{wL^4}{EI} \quad (4.5)$$

Solving for the moment of inertia of the T-section gives

$$I_T = -5.3406 \times 10^{-3} \frac{wL^4}{E \nu_{FE} (3L/8)} \quad (4.6)$$

In Equations (4.4) and (4.6),  $I_T$  represents the moment of inertia of the transformed T-section. In a beam-and-slab floor system, the web dimensions and the slab thickness, and hence the flange thickness of the T-section are known in advance. However, the effective flange width  $b_e$  remains as an unknown to be determined.

Depending on the type of loading, the numerical value for  $I_T$  can easily be computed either from Eq. (4.4) or Eq. (4.6) using the input data and the finite element displacement results. The computed value of the moment of inertia is then substituted into the appropriate expression for the moment of inertia calculations given in Equations (3.9) and (3.11). As a sample case, for instance, for the case of point load, and when Eq. (3.9) applies, the resulting expression for the effective flange width is

$$\frac{b_e h}{3} (3z^2 + 3hz + h^2) + \frac{b_w}{3} [z^3 + (d - z)^3] = -\frac{7PL^3}{768 E \nu_{FE} (L/2)} \quad (4.7)$$

It should be remembered that in the above equation, the distance  $z$  between the neutral axis and the bottom edge of the flange is also a function of the effective flange width  $b_e$ . The moment of inertia expression given in Eq. (4.7) can be solved for the unknown effective width  $b_e$  by using Mathcad program. The results are given for both loading types in Tables 4.2 and 4.3.

Table 4.2 Effective flange width results for loading at midspan

Beam No	S (cm)	L (cm)	D (cm)	$b_w$ (cm)	h (cm)	S/L	L/D	$b_w/D$	h/D	$v @ x=L/2$ (cm)	$b_e$ (cm)	Inertia (cm <sup>4</sup> )	$b_e/S$
1	120	600	60	39	12	0,2	10	0,65	0,2	0,0984	83,82	960365,85	0,70
2	180	900	60	39	12	0,2	15	0,65	0,2	0,6123	138,59	1171989,83	0,77
3	240	1200	60	39	12	0,2	20	0,65	0,2	2,3000	191,21	1314782,61	0,80
4	120	600	60	42	12	0,2	10	0,7	0,2	0,0936	85,15	1009615,38	0,71
5	180	900	60	42	12	0,2	15	0,7	0,2	0,5823	140,12	1232370,56	0,78
6	240	1200	60	42	12	0,2	20	0,7	0,2	2,1848	192,69	1384108,39	0,80
7	120	600	60	45	12	0,2	10	0,75	0,2	0,0893	86,51	1058230,68	0,72
8	180	900	60	45	12	0,2	15	0,75	0,2	0,5558	141,62	1291128,78	0,79
9	240	1200	60	45	12	0,2	20	0,75	0,2	2,0835	194,14	1451403,89	0,81
10	80	400	40	26	12	0,2	10	0,65	0,3	0,0635	56,40	195975,50	0,70
11	120	600	40	26	12	0,2	15	0,65	0,3	0,3971	93,88	237975,32	0,78
12	160	800	40	26	12	0,2	20	0,65	0,3	1,4987	131,41	265711,77	0,82
13	80	400	40	28	12	0,2	10	0,7	0,3	0,0604	57,32	206033,85	0,72
14	120	600	40	28	12	0,2	15	0,7	0,3	0,3773	94,73	250463,82	0,79
15	160	800	40	28	12	0,2	20	0,7	0,3	1,4225	131,91	279945,32	0,82
16	80	400	40	30	12	0,2	10	0,75	0,3	0,0577	58,12	215674,95	0,73
17	120	600	40	30	12	0,2	15	0,75	0,3	0,3599	95,56	262572,94	0,80
18	160	800	40	30	12	0,2	20	0,75	0,3	1,3554	132,49	293804,21	0,83
19	60	300	30	19,5	12	0,2	10	0,65	0,4	0,0467	43,97	63236,31	0,73
20	90	450	30	19,5	12	0,2	15	0,65	0,4	0,2914	74,62	76957,08	0,83
21	120	600	30	19,5	12	0,2	20	0,65	0,4	1,0913	105,84	86593,97	0,88
22	60	300	30	21	12	0,2	10	0,7	0,4	0,0445	44,42	66362,36	0,74
23	90	450	30	21	12	0,2	15	0,7	0,4	0,2774	74,84	80841,00	0,83

Table 4.2 Effective flange width results for loading at midspan (Continued)

Beam No	S (cm)	L (cm)	D (cm)	$b_{w,eff}$ (cm)	h (cm)	S/L	L/D	$b_w/D$	h/D	$v_{@x=L/2}$ (cm)	$b_e$ (cm)	Inertia (cm <sup>4</sup> )	$b_e/S$
24	120	600	30	21	12	0,2	20	0,7	0,4	1,0392	105,65	90935,33	0,88
25	60	300	30	22,5	12	0,2	10	0,75	0,4	0,0425	45,00	69485,29	0,75
26	90	450	30	22,5	12	0,2	15	0,75	0,4	0,2651	75,03	84591,83	0,83
27	120	600	30	22,5	12	0,2	20	0,75	0,4	0,9929	105,53	95175,75	0,88
28	150	600	60	39	12	0,25	10	0,65	0,2	0,1165	95,74	1013948,50	0,64
29	225	900	60	39	12	0,25	15	0,65	0,2	0,7281	158,73	1231989,73	0,71
30	300	1200	60	39	12	0,25	20	0,65	0,2	2,7465	219,70	1376297,11	0,73
31	150	600	60	42	12	0,25	10	0,7	0,2	0,1107	97,42	1067073,17	0,65
32	225	900	60	42	12	0,25	15	0,7	0,2	0,6915	160,68	1297196,99	0,71
33	300	1200	60	42	12	0,25	20	0,7	0,2	2,6053	221,55	1450888,57	0,74
34	150	600	60	45	12	0,25	10	0,75	0,2	0,1055	99,19	1119668,25	0,66
35	225	900	60	45	12	0,25	15	0,75	0,2	0,6592	162,60	1360758,07	0,72
36	300	1200	60	45	12	0,25	20	0,75	0,2	2,4814	223,34	1523333,60	0,74
37	100	400	40	26	12	0,25	10	0,65	0,3	0,0751	64,67	207131,23	0,65
38	150	600	40	26	12	0,25	15	0,65	0,3	0,4710	109,61	250796,18	0,73
39	200	800	40	26	12	0,25	20	0,65	0,3	1,7816	155,44	279399,29	0,78
40	100	400	40	28	12	0,25	10	0,7	0,3	0,0713	65,89	218170,48	0,66
41	150	600	40	28	12	0,25	15	0,7	0,3	0,4471	110,49	264202,64	0,74
42	200	800	40	28	12	0,25	20	0,7	0,3	1,6899	155,72	294560,49	0,78
43	100	400	40	30	12	0,25	10	0,75	0,3	0,0680	66,93	228758,17	0,67
44	150	600	40	30	12	0,25	15	0,75	0,3	0,4261	111,35	277223,66	0,74
45	200	800	40	30	12	0,25	20	0,75	0,3	1,6092	156,10	309332,45	0,78
46	75	300	30	19,5	12	0,25	10	0,65	0,4	0,0548	51,70	67361,43	0,69

Table 4.2 Effective flange width results for loading at midspan (Continued)

Beam No	S (cm)	L (cm)	D (cm)	$b_{w,x}$ (cm)	h (cm)	S/L	L/D	$b_{w,D}$	h/D	$v @ x=L/2$ (cm)	$b_e$ (cm)	Inertia (cm <sup>4</sup> )	$b_e/S$
47	112,5	450	30	19,5	12	0,25	15	0,65	0,4	0,3411	90,46	82180,05	0,80
48	150	600	30	19,5	12	0,25	20	0,65	0,4	1,2741	130,20	92712,50	0,87
49	75	300	30	21	12	0,25	10	0,7	0,4	0,0521	52,37	70852,33	0,70
50	112,5	450	30	21	12	0,25	15	0,7	0,4	0,3248	90,43	86304,24	0,80
51	150	600	30	21	12	0,25	20	0,7	0,4	1,2143	129,56	97278,27	0,86
52	75	300	30	22,5	12	0,25	10	0,75	0,4	0,0498	52,79	74124,62	0,70
53	112,5	450	30	22,5	12	0,25	15	0,75	0,4	0,3104	90,41	90308,04	0,80
54	150	600	30	22,5	12	0,25	20	0,75	0,4	1,1609	129,05	101752,95	0,86
55	180	600	60	39	12	0,3	10	0,65	0,2	0,1350	104,42	1050000,00	0,58
56	270	900	60	39	12	0,3	15	0,65	0,2	0,8460	173,82	1272357,05	0,64
57	360	1200	60	39	12	0,3	20	0,65	0,2	3,1988	241,63	1418031,76	0,67
58	180	600	60	42	12	0,3	10	0,7	0,2	0,1281	106,55	1106557,38	0,59
59	270	900	60	42	12	0,3	15	0,7	0,2	0,8027	176,10	1340991,73	0,65
60	360	1200	60	42	12	0,3	20	0,7	0,2	3,0321	243,61	1495992,88	0,68
61	180	600	60	45	12	0,3	10	0,75	0,2	0,1220	108,60	1161885,25	0,60
62	270	900	60	45	12	0,3	15	0,75	0,2	0,7646	178,31	1407813,32	0,66
63	360	1200	60	45	12	0,3	20	0,75	0,2	2,8857	245,59	1571888,97	0,68
64	120	400	40	26	12	0,3	10	0,65	0,3	0,0867	71,42	215301,81	0,60
65	180	600	40	26	12	0,3	15	0,65	0,3	0,5444	123,13	260378,40	0,68
66	240	800	40	26	12	0,3	20	0,65	0,3	2,0599	177,14	289981,71	0,74
67	120	400	40	28	12	0,3	10	0,7	0,3	0,0822	72,89	227088,40	0,61
68	180	600	40	28	12	0,3	15	0,7	0,3	0,5167	123,82	274337,14	0,69
69	240	800	40	28	12	0,3	20	0,7	0,3	1,9539	176,90	305713,36	0,74

Table 4.2 Effective flange width results for loading at midspan (Continued)

Beam No	S (cm)	L (cm)	D (cm)	$b_{w,1}$ (cm)	h (cm)	S/L	L/D	$b_{w,2}/D$	h/D	$v @ x=L/2$ (cm)	$b_e$ (cm)	Inertia (cm <sup>4</sup> )	$b_e/S$
70	120	400	40	30	12	0,3	10	0,75	0,3	0,0783	74,15	238399,32	0,62
71	180	600	40	30	12	0,3	15	0,75	0,3	0,4921	124,72	288051,21	0,69
72	240	800	40	30	12	0,3	20	0,75	0,3	1,8603	176,91	321095,16	0,74
73	90	300	30	19,5	12	0,3	10	0,65	0,4	0,0626	58,98	70761,78	0,66
74	135	450	30	19,5	12	0,3	15	0,65	0,4	0,3884	105,89	86606,44	0,78
75	180	600	30	19,5	12	0,3	20	0,65	0,4	1,4450	154,35	98096,89	0,86
76	90	300	30	21	12	0,3	10	0,7	0,4	0,0596	59,37	74323,62	0,66
77	135	450	30	21	12	0,3	15	0,7	0,4	0,3702	105,40	90864,23	0,78
78	180	600	30	21	12	0,3	20	0,7	0,4	1,3789	153,14	102799,33	0,85
79	90	300	30	22,5	12	0,3	10	0,75	0,4	0,0569	59,91	77850,40	0,67
80	135	450	30	22,5	12	0,3	15	0,75	0,4	0,3539	105,11	95049,28	0,78
81	180	600	30	22,5	12	0,3	20	0,75	0,4	1,3195	152,15	107427,06	0,85

Table 4.3 Effective flange width results for uniform loading

Beam No	S (cm)	L (cm)	D (cm)	$b_w$ (cm)	h (cm)	S/L	L/D	$b_w/D$	h/D	$v @ x=3L/8$ (cm)	$b_e$ (cm)	Inertia (cm <sup>4</sup> )	$b_e/S$
1	120	600	60	39	12	0,2	10	0,65	0,2	0,0578	83,32	957981,68	0,69
2	180	900	60	39	12	0,2	15	0,65	0,2	0,3570	140,43	1177804,26	0,78
3	240	1200	60	39	12	0,2	20	0,65	0,2	1,3402	194,39	1322103,35	0,81
4	120	600	60	42	12	0,2	10	0,7	0,2	0,0550	84,56	1006751,65	0,70
5	180	900	60	42	12	0,2	15	0,7	0,2	0,3396	141,85	1238151,12	0,79
6	240	1200	60	42	12	0,2	20	0,7	0,2	1,2731	195,80	1391786,12	0,82
7	120	600	60	45	12	0,2	10	0,75	0,2	0,0525	85,82	1054692,21	0,72
8	180	900	60	45	12	0,2	15	0,75	0,2	0,3242	143,29	1296965,21	0,80
9	240	1200	60	45	12	0,2	20	0,75	0,2	1,2142	197,15	1459300,70	0,82
10	80	400	40	26	12	0,2	10	0,65	0,3	0,0374	55,70	194965,22	0,70
11	120	600	40	26	12	0,2	15	0,65	0,3	0,2319	94,79	238772,49	0,79
12	160	800	40	26	12	0,2	20	0,65	0,3	0,8748	133,05	266728,82	0,83
13	80	400	40	28	12	0,2	10	0,7	0,3	0,0355	56,90	205399,98	0,71
14	120	600	40	28	12	0,2	15	0,7	0,3	0,2203	95,67	251345,17	0,80
15	160	800	40	28	12	0,2	20	0,7	0,3	0,8303	133,53	281024,18	0,83
16	80	400	40	30	12	0,2	10	0,75	0,3	0,0339	57,76	215094,37	0,72
17	120	600	40	30	12	0,2	15	0,75	0,3	0,2102	96,41	263422,17	0,80
18	160	800	40	30	12	0,2	20	0,75	0,3	0,7911	134,10	294949,28	0,84
19	60	300	30	19,5	12	0,2	10	0,65	0,4	0,0276	43,04	62694,00	0,72
20	90	450	30	19,5	12	0,2	15	0,65	0,4	0,1706	74,80	77021,56	0,83
21	120	600	30	19,5	12	0,2	20	0,65	0,4	0,6385	106,31	86720,97	0,89
22	60	300	30	21	12	0,2	10	0,7	0,4	0,0262	43,90	66044,06	0,73
23	90	450	30	21	12	0,2	15	0,7	0,4	0,1624	75,03	80910,58	0,83

Table 4.3 Effective flange width results for uniform loading

Beam No	S (cm)	L (cm)	D (cm)	$b_w$ (cm)	h (cm)	S/L	L/D	$b_w/D$	h/D	$v @ x=3L/8$ (cm)	$b_e$ (cm)	Inertia (cm <sup>4</sup> )	$b_e/S$
24	120	600	30	21	12	0,2	20	0,7	0,4	0,6080	106,12	91071,28	0,88
25	60	300	30	22,5	12	0,2	10	0,75	0,4	0,0251	44,15	68938,42	0,74
26	90	450	30	22,5	12	0,2	15	0,75	0,4	0,1551	75,34	84718,75	0,84
27	120	600	30	22,5	12	0,2	20	0,75	0,4	0,5808	106,06	95336,33	0,88
28	150	600	60	39	12	0,25	10	0,65	0,2	0,0684	95,26	1011903,16	0,64
29	225	900	60	39	12	0,25	15	0,65	0,2	0,4243	161,16	1238734,74	0,72
30	300	1200	60	39	12	0,25	20	0,65	0,2	1,5998	223,81	1384456,58	0,75
31	150	600	60	42	12	0,25	10	0,7	0,2	0,0650	96,92	1064833,48	0,65
32	225	900	60	42	12	0,25	15	0,7	0,2	0,4030	163,06	1304206,33	0,72
33	300	1200	60	42	12	0,25	20	0,7	0,2	1,5176	225,56	1459444,93	0,75
34	150	600	60	45	12	0,25	10	0,75	0,2	0,0620	98,48	1116357,68	0,66
35	225	900	60	45	12	0,25	15	0,75	0,2	0,3843	164,82	1367668,88	0,73
36	300	1200	60	45	12	0,25	20	0,75	0,2	1,4455	227,26	1532240,49	0,76
37	100	400	40	26	12	0,25	10	0,65	0,3	0,0442	63,95	206213,21	0,64
38	150	600	40	26	12	0,25	15	0,65	0,3	0,2751	110,68	251596,42	0,74
39	200	800	40	26	12	0,25	20	0,65	0,3	1,0404	157,26	280342,15	0,79
40	100	400	40	28	12	0,25	10	0,7	0,3	0,0419	65,41	217532,79	0,65
41	150	600	40	28	12	0,25	15	0,7	0,3	0,2611	111,59	265086,85	0,74
42	200	800	40	28	12	0,25	20	0,7	0,3	0,9868	157,52	295569,49	0,79
43	100	400	40	30	12	0,25	10	0,75	0,3	0,0400	66,30	227865,60	0,66
44	150	600	40	30	12	0,25	15	0,75	0,3	0,2488	112,49	278192,03	0,75
45	200	800	40	30	12	0,25	20	0,75	0,3	0,9396	157,90	310417,16	0,79
46	75	300	30	19,5	12	0,25	10	0,65	0,4	0,0323	50,91	66964,18	0,68

Table 4.3 Effective flange width results for uniform loading

Beam No	S (cm)	L (cm)	D (cm)	$b_{w,x}$ (cm)	h (cm)	S/L	L/D	$b_{w,D}$	h/D	$v @ x=3L/8$ (cm)	$b_e$ (cm)	Inertia (cm <sup>4</sup> )	$b_{e,S}$
47	112,5	450	30	19,5	12	0,25	15	0,65	0,4	0,1999	90,41	82165,32	0,80
48	150	600	30	19,5	12	0,25	20	0,65	0,4	0,7464	130,27	92730,68	0,87
49	75	300	30	21	12	0,25	10	0,7	0,4	0,0308	51,18	70225,42	0,68
50	112,5	450	30	21	12	0,25	15	0,7	0,4	0,1903	90,44	86310,29	0,80
51	150	600	30	21	12	0,25	20	0,7	0,4	0,7112	129,73	97320,27	0,86
52	75	300	30	22,5	12	0,25	10	0,75	0,4	0,0294	51,80	73569,49	0,69
53	112,5	450	30	22,5	12	0,25	15	0,75	0,4	0,1818	90,52	90345,70	0,80
54	150	600	30	22,5	12	0,25	20	0,75	0,4	0,6798	129,29	101815,50	0,86
55	180	600	60	39	12	0,3	10	0,65	0,2	0,0793	103,77	1047377,19	0,58
56	270	900	60	39	12	0,3	15	0,65	0,2	0,4931	176,46	1279079,66	0,65
57	360	1200	60	39	12	0,3	20	0,65	0,2	1,8642	245,93	1425718,46	0,68
58	180	600	60	42	12	0,3	10	0,7	0,2	0,0753	105,70	1103014,76	0,59
59	270	900	60	42	12	0,3	15	0,7	0,2	0,4680	178,58	1347679,87	0,66
60	360	1200	60	42	12	0,3	20	0,7	0,2	1,7670	247,84	1504145,08	0,69
61	180	600	60	45	12	0,3	10	0,75	0,2	0,0717	107,80	1158396,25	0,60
62	270	900	60	45	12	0,3	15	0,75	0,2	0,4458	180,76	1414791,79	0,67
63	360	1200	60	45	12	0,3	20	0,75	0,2	1,6817	249,75	1580439,06	0,69
64	120	400	40	26	12	0,3	10	0,65	0,3	0,0510	70,70	214461,74	0,59
65	180	600	40	26	12	0,3	15	0,65	0,3	0,3183	123,98	260939,40	0,69
66	240	800	40	26	12	0,3	20	0,65	0,3	1,2042	178,61	290650,69	0,74
67	120	400	40	28	12	0,3	10	0,7	0,3	0,0484	71,98	225982,41	0,60
68	180	600	40	28	12	0,3	15	0,7	0,3	0,3020	124,79	275023,22	0,69
69	240	800	40	28	12	0,3	20	0,7	0,3	1,1420	178,46	306481,23	0,74

Table 4.3 Effective flange width results for uniform loading

Beam No	S (cm)	L (cm)	D (cm)	$b_{xx}$ (cm)	h (cm)	S/L	L/D	$b_{xx}/D$	h/D	$v @ x=3L/8$ (cm)	$b_e$ (cm)	Inertia (cm <sup>4</sup> )	$b_{e}/S$
70	120	400	40	30	12	0,3	10	0,75	0,3	0,0461	73,26	237257,02	0,61
71	180	600	40	30	12	0,3	15	0,75	0,3	0,2877	125,56	288693,12	0,70
72	240	800	40	30	12	0,3	20	0,75	0,3	1,0872	178,49	321929,32	0,74
73	90	300	30	19,5	12	0,3	10	0,65	0,4	0,0370	57,60	70149,50	0,64
74	135	450	30	19,5	12	0,3	15	0,65	0,4	0,2280	105,30	86446,57	0,78
75	180	600	30	19,5	12	0,3	20	0,65	0,4	0,8478	153,74	97967,69	0,85
76	90	300	30	21	12	0,3	10	0,7	0,4	0,0352	58,13	73736,69	0,65
77	135	450	30	21	12	0,3	15	0,7	0,4	0,2172	104,99	90745,02	0,78
78	180	600	30	21	12	0,3	20	0,7	0,4	0,8088	152,66	102691,66	0,85
79	90	300	30	22,5	12	0,3	10	0,75	0,4	0,0336	58,70	77247,96	0,65
80	135	450	30	22,5	12	0,3	15	0,75	0,4	0,2076	104,76	94941,32	0,78
81	180	600	30	22,5	12	0,3	20	0,75	0,4	0,7738	151,77	107336,54	0,84

## CHAPTER 5

### MULTIPLE NONLINEAR REGRESSION ANALYSIS

#### 5.1 Multiple Nonlinear Regression Analysis

The basic idea of nonlinear regression is the same as that of linear regression, namely to relate a response  $Y$  to a vector of predictor variables in the form  $x = (x_1, \dots, x_k)^T$ . Nonlinear regression is characterized by the fact that the prediction equation depends on one or more unknown parameters. Whereas linear regression is often used for building a purely empirical model, nonlinear regression usually arises when there are physical reasons for believing that the relationship between the response and the predictors follows a particular functional form. A nonlinear regression model has the form

$$Y_i = f(x_i, \theta) + \varepsilon_i \quad i = 1, \dots, n \quad (5.1)$$

where  $Y_i$  are responses,  $f$  is a known function of the covariate vector  $x_i = (x_{i1}, \dots, x_{ik})^T$  and the parameter vector  $\theta = (\theta_1, \dots, \theta_p)^T$  and  $\varepsilon_i$  are random errors.

Nonlinear regression analysis estimates the coefficients of the nonlinear equation, involving one or more independent variables that best predict the value of the dependent variable.

In most empirical studies, the value of dependent variable  $Y$  is not uniquely determined when the level of independent variable  $X$  is specified. Such relations are called statistical relations. Statistical relations can be either linear or nonlinear. In this study, the model that defines the relation between dependent and independent variables is selected as nonlinear so as to make a comparison with the previous studies.

## 5.2 Nonlinear Regression Model

The statistical model used in this study is nonlinear and the regression equation takes the form as;

$$Y = \beta_1 \times A_1^{\beta_2} \times A_2^{\beta_3} \times A_3^{\beta_4} \times A_4^{\beta_5} \quad (5.2)$$

This form is considered to fit the model in the same format with the result of those studies done by Loo and Sutandi (1986), Utku and Aygar (2002). In the above equation,  $\beta_1$  to  $\beta_5$  represent constant values of the regression model, which are called as the estimates of the model, and  $A_1$  to  $A_4$  represent the set of independent predictor variables.

This statistical technique allows us to predict the ratio of effective flange width to beam spacing ( $b_e/S$ ) on the basis of some independent variables. There are four independent variables which influence this ratio. These independent variables are obtained as the ratios of beam geometric parameters. Four independent variables from  $A_1$  to  $A_4$  are “S/L”, “L/D”, “h/D” and “ $b_w/D$ ” respectively.

The effective flange width values are given in Table 4.2 and 4.3 for 81 combinations of these four independent variables and for each loading condition. Then, nonlinear regression analyses were carried out on this

available data using the software SPSS, “Statistical Package for the Social Sciences” (2006).

For the determination of the relation equation, the format of the relationship is defined by using nonlinear regression in SPSS program. Since the program will use an iterative method for obtaining such an equation, first values of all parameters used in this study are assigned to initial values equal to zero. When the iteration is completed, the estimated values of  $\beta_1$  to  $\beta_5$  are given as output with their correlations with respect to each other.

For nonlinear regression model of the load at midspan case, 26 iterations were performed using SPSS program, resulting in the parameter estimates as given in Table 5.1.

Table 5.1 Estimate values of parameters (Load at midspan)

Parameter Estimates				
Parameter	Estimate	Std. Error	95% Confidence Interval	
			Lower Bound	Upper Bound
B1	,322	,018	,287	,357
B2	-,295	,022	-,338	-,251
B3	,246	,013	,220	,272
B4	,091	,062	-,033	,215
B5	,170	,013	,144	,196

The use of the above parameters in Eq. (5.2) led to the following nonlinear equation for effective flange width,  $b_e$ , for point load:

$$\frac{b_e}{S} = 0.322 \times \left(\frac{S}{L}\right)^{-0.2947} \times \left(\frac{L}{D}\right)^{0.2463} \times \left(\frac{b_w}{D}\right)^{0.0913} \times \left(\frac{h}{D}\right)^{0.1698} \quad (5.3)$$

Analysis of variance is also performed for the parameters by SPSS, giving 95.1 % value of variance which illustrates that model is a good representative of the finite element analysis results.

For the nonlinear model of uniformly distributed load case, the parameter estimates obtained after 26 iterations are given in Table 5.2.

Table 5.2 Estimate values of parameters (Uniformly distributed load)

Parameter Estimates				
Parameter	Estimate	Std. Error	95% Confidence Interval	
			Lower Bound	Upper Bound
B1	,286	,015	,255	,316
B2	-,306	,021	-,349	-,263
B3	,275	,013	,249	,300
B4	,087	,061	-,035	,208
B5	,147	,013	,122	,173

For the uniformly distributed load case, the substitution the above parameters into Eq. (5.2) again led to the following nonlinear equation for effective flange width  $b_e$ :

$$\frac{b_e}{S} = 0.2858 \times \left(\frac{S}{L}\right)^{-0.3058} \times \left(\frac{L}{D}\right)^{0.2746} \times \left(\frac{b_w}{D}\right)^{0.086} \times \left(\frac{h}{D}\right)^{0.1473} \quad (5.4)$$

Analysis of variance for this model was obtained as 95.6 % which is an indication of a good correlation between the formulas and the finite element analyses.

### 5.3. Comparison with the Code Equations

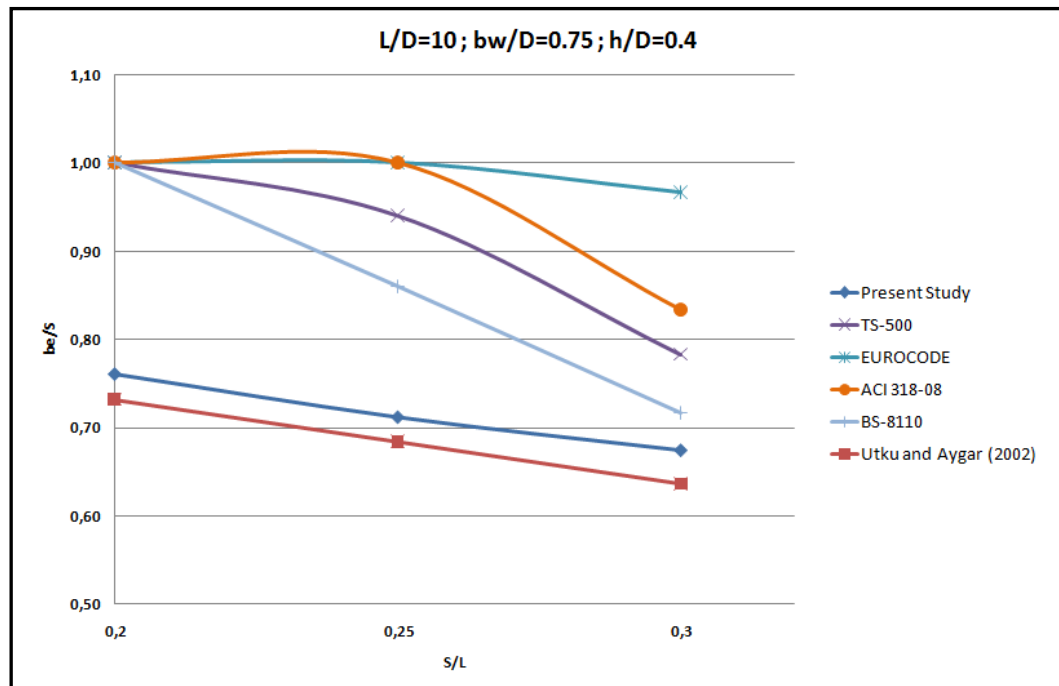
The design formulas defined in Equations (5.3) and (5.4) for effective flange width are compared with the code equations given in ACI, Eurocode, BS8110 and TS500. Moreover, these formulas are also compared with the expressions given by Utku and Aygar (2002). In Figure 5.1 the  $b_e/S$  ratios permitted by various codes for the assumed cases of  $L/D$ ,  $b_w/D$  and  $h/D$  are compared with the proposed formulas against  $S/L$ . Three of the typical curves for load at midspan are shown in Figure 5.1. The cases considered and the corresponding values of parameters are as follows:

Case 1:  $L/D = 10$ ,  $b_w/D = 0.75$ ,  $h/D = 0.4$

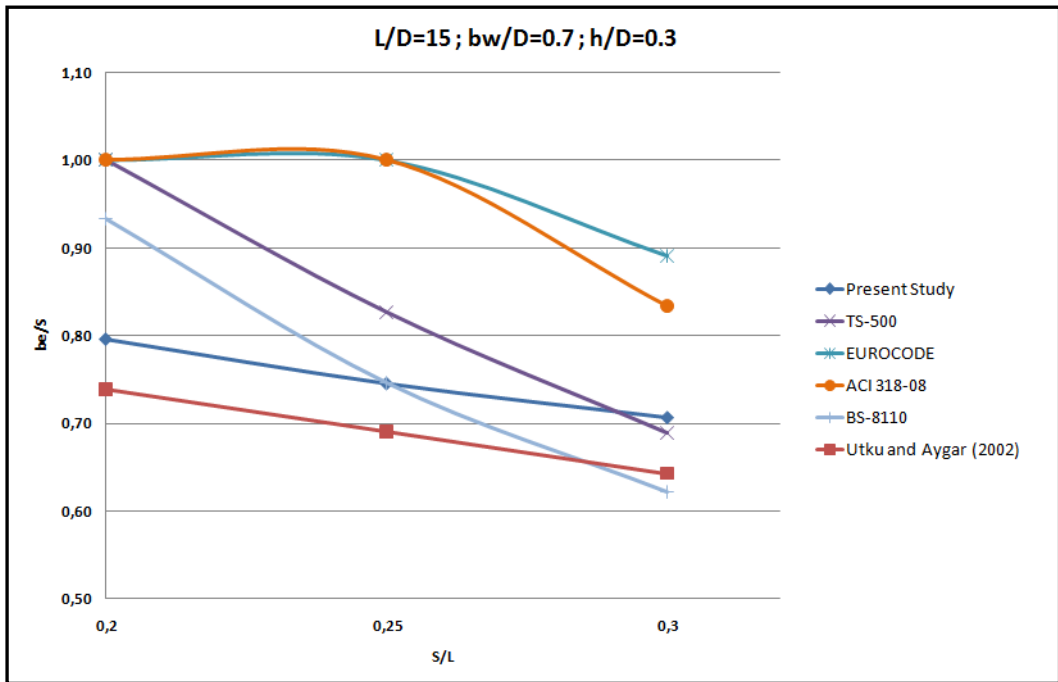
Case 2:  $L/D = 15$ ,  $b_w/D = 0.7$ ,  $h/D = 0.3$

Case 3:  $L/D = 20$ ,  $b_w/D = 0.65$ ,  $h/D = 0.2$

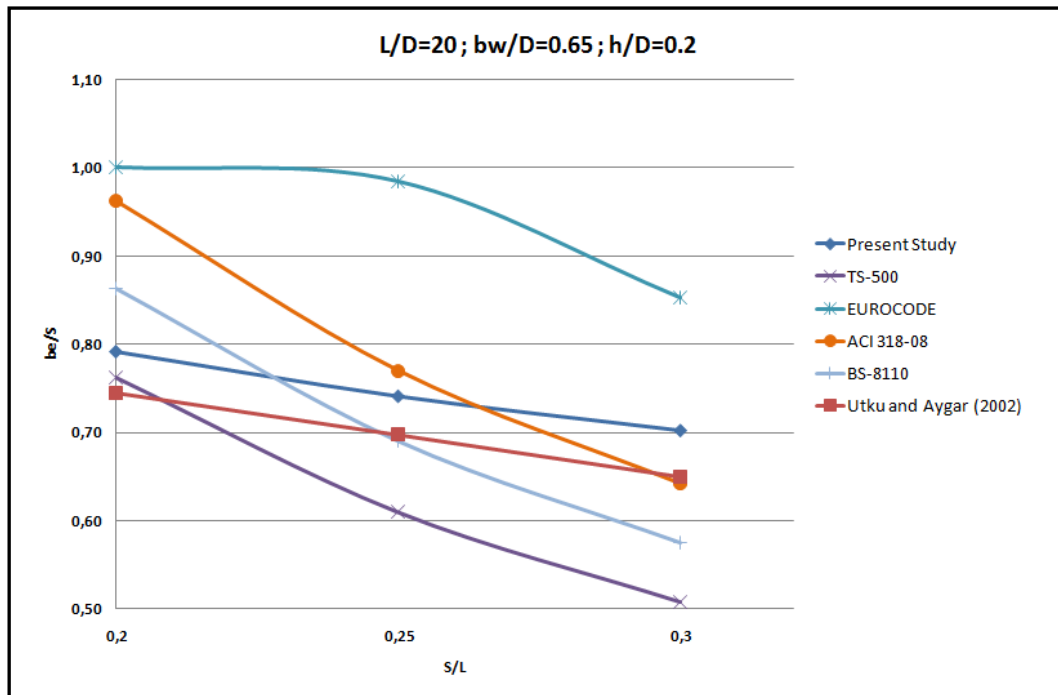
It should be noted that with the chosen values of the parameters, the change from Case1 to Case 3 represents the change from stubby beams to slender beams.



(a)  $L/D = 10$ ,  $b_w/D = 0.75$ ,  $h/D = 0.4$



(b)  $L/D = 15$  ,  $b_w/D = 0.7$  ,  $h/D = 0.3$



(c)  $L/D = 20$  ,  $b_w/D = 0.65$  ,  $h/D = 0.2$

Figure 5.1 Comparison of design formulas with the code equations for load at midspan

It is observed from Figure 5.1 that for the concentrated load case, the codes considered here are unsafe for the stubby beams. As the beam gets slender, this trend changes and smaller effective flange width values are obtained for increasing values of the beam spacing. However, for all cases the recommendations given by Eurocode give overestimated results.

The results for  $b_e/S$  obtained from Eq. (5.3) for three cases are shown in Figure 5.2 over a larger interval of  $S/L$ . The comparison of the three cases shows that as the beam spacing  $S$  increases,  $b_e/S$  decreases. Moreover, for the same value of the beam spacing  $S$ , the ratio  $b_e/S$  increases as the span length  $L$  increases. It is also observed from Figure 5.2 that graphs are very close to each other, and even Cases 2 and 3 happen to lie on top of each other. Therefore, it can be concluded that the beam spacing  $S$  and the beam span length  $L$  affect the effective flange width more significantly than the other parameters.

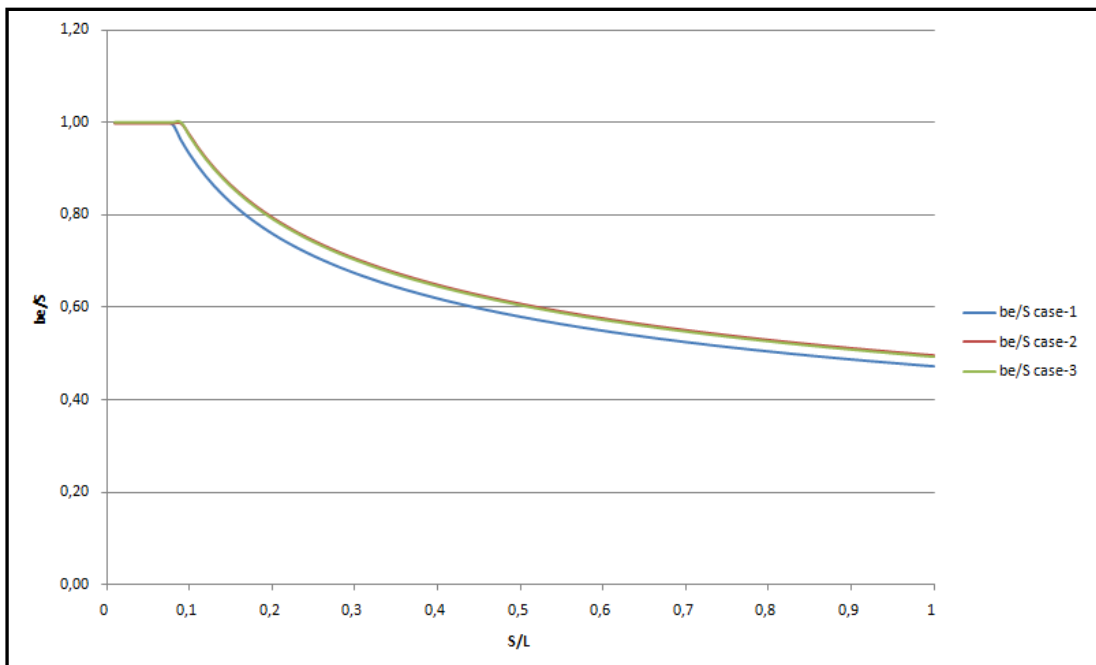
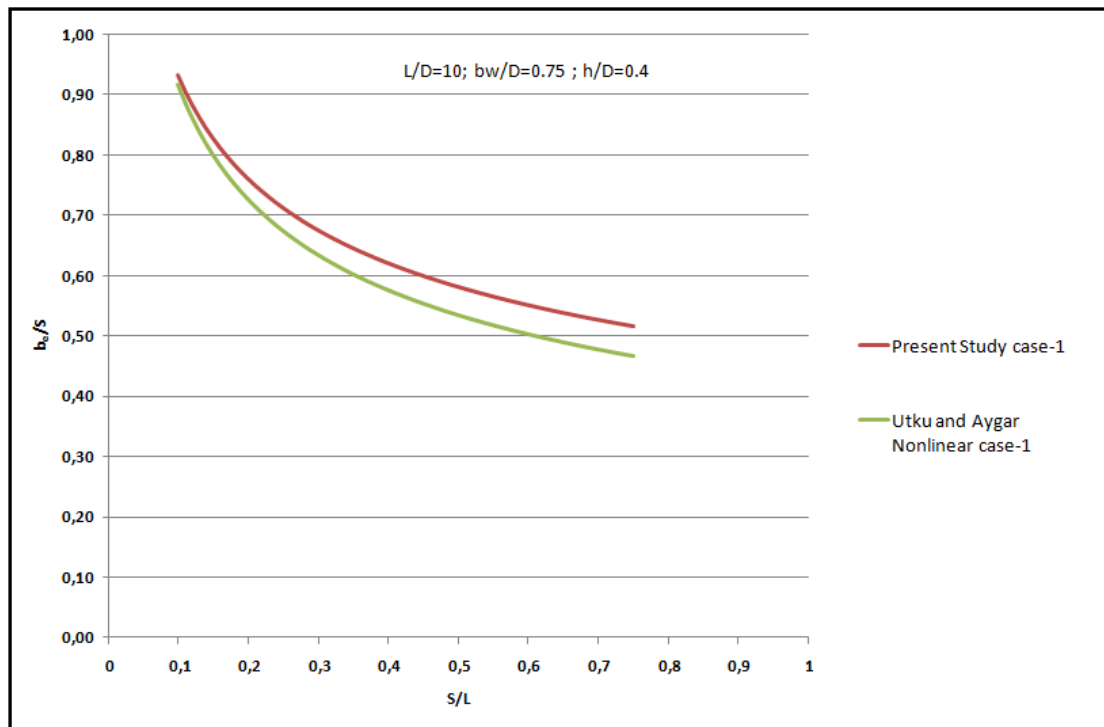
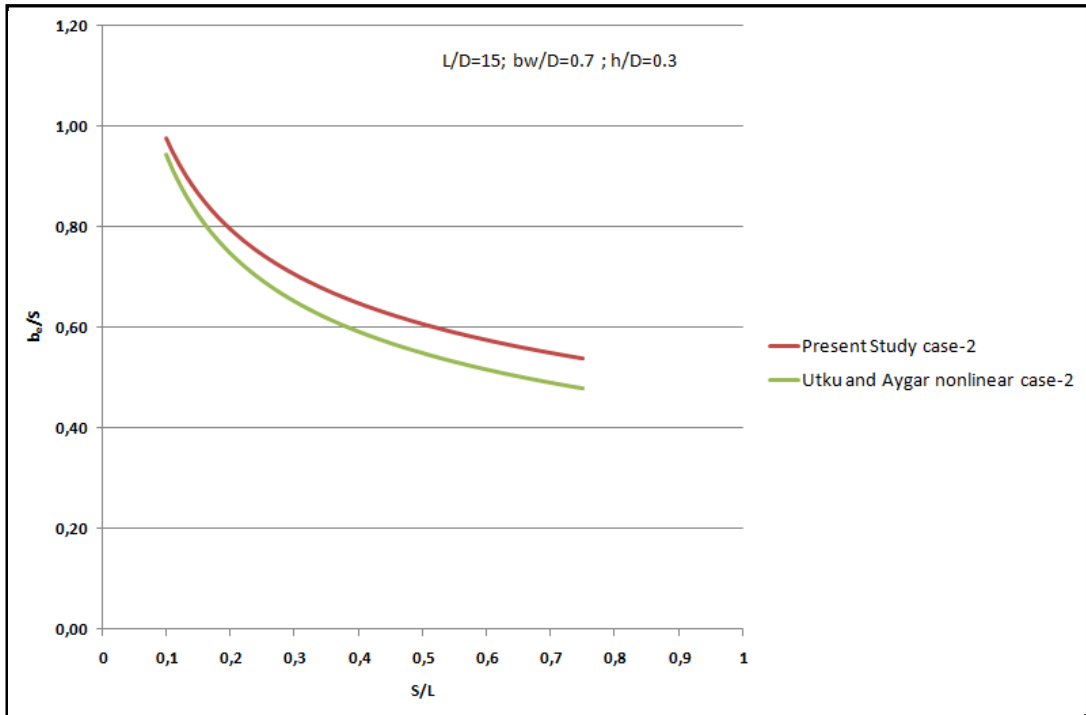


Figure 5.2 “S/L” versus “ $b_e/S$ ” for Case1, Case2 and Case3

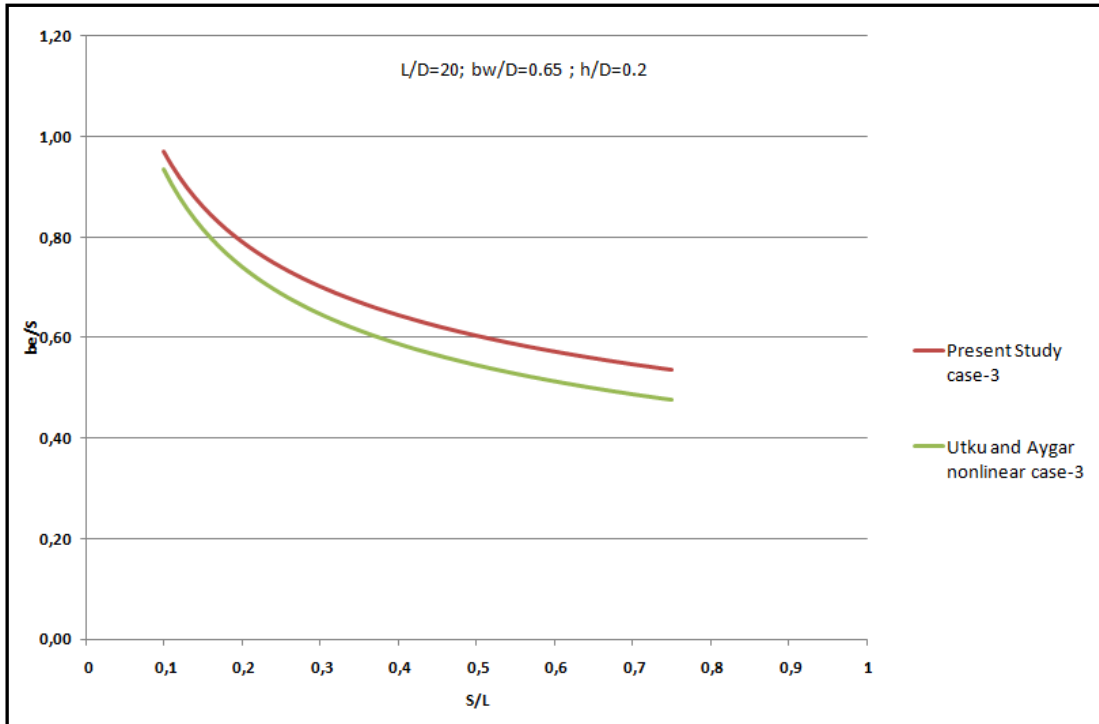
In addition to these comparison curves, results of each three cases are also compared with those of Utku and Aygar (2002) in Figure 5.3. It is observed that the results of the present work compare well with results based on stress criterion.



(a)  $L/D = 10$  ,  $b_w/D = 0.75$  ,  $h/D = 0.4$



(b)  $L/D = 15$  ,  $b_w/D = 0.7$  ,  $h/D = 0.3$

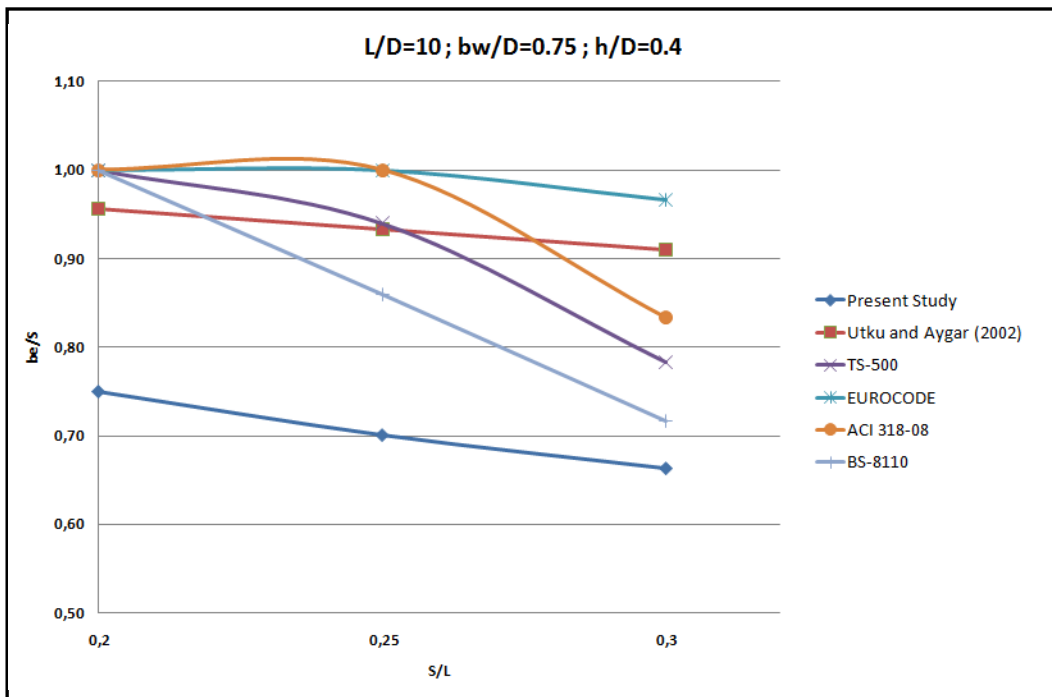


(c)  $L/D = 20$  ,  $b_w/D = 0.65$  ,  $h/D = 0.2$

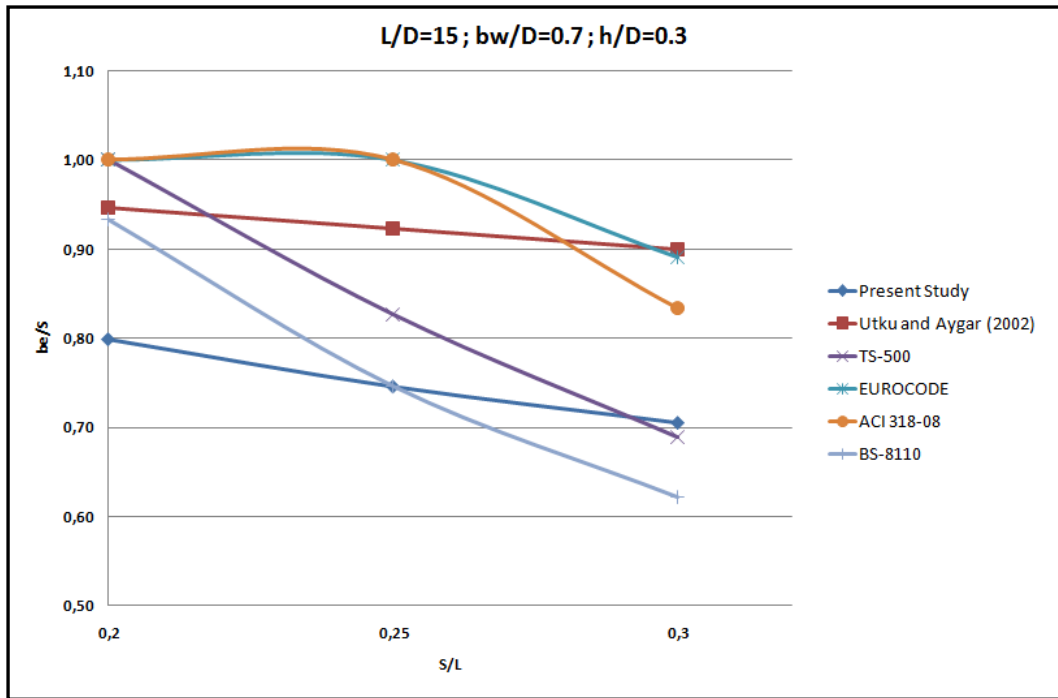
Figure 5.3 Effective flange width based on stress criterion and deflection consideration (Point load)

Similar curves are also prepared for uniformly distributed load case and these curves are represented in Figures 5.4, 5.5 and 5.6.

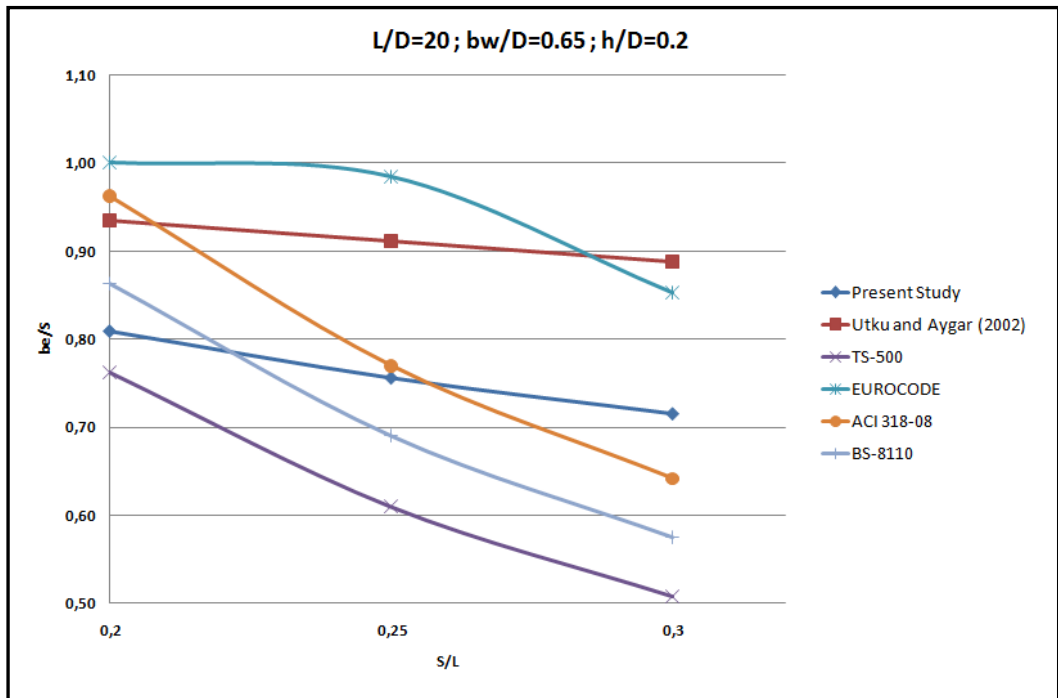
It is observed from Figure 5.4a that for stubby beams, the proposed formula gives rather conservative results with respect to the code equations. However, as the beams get slender all codes give very conservative assessments of  $b_e$  for uniformly distributed load case except for Eurocode which gives consistently overestimated results for all cases. For most of the beams under a uniform distributed load, Eurocode values of  $b_e/S$  are very close to unity.



(a)  $L/D = 10$  ,  $b_w/D = 0.75$  ,  $h/D = 0.4$



(b)  $L/D = 15, b_w/D = 0.7, h/D = 0.3$



(c)  $L/D = 20, b_w/D = 0.65, h/D = 0.2$

Figure 5.4 Comparison of design formulas with the code equations for uniformly distributed load

The results for  $b_e/S$  obtained from Eq. (5.4) for the three cases again are shown in Figure 5.5 over a larger interval of  $S/L$ . From the comparison of Figure 5.2 for point load case and Figure 5.4 for uniform loading, a similar trend is observed for the variation of effective flange width against the beam spacing, except a very small increase in the  $b_e/S$  results for the uniform loading.

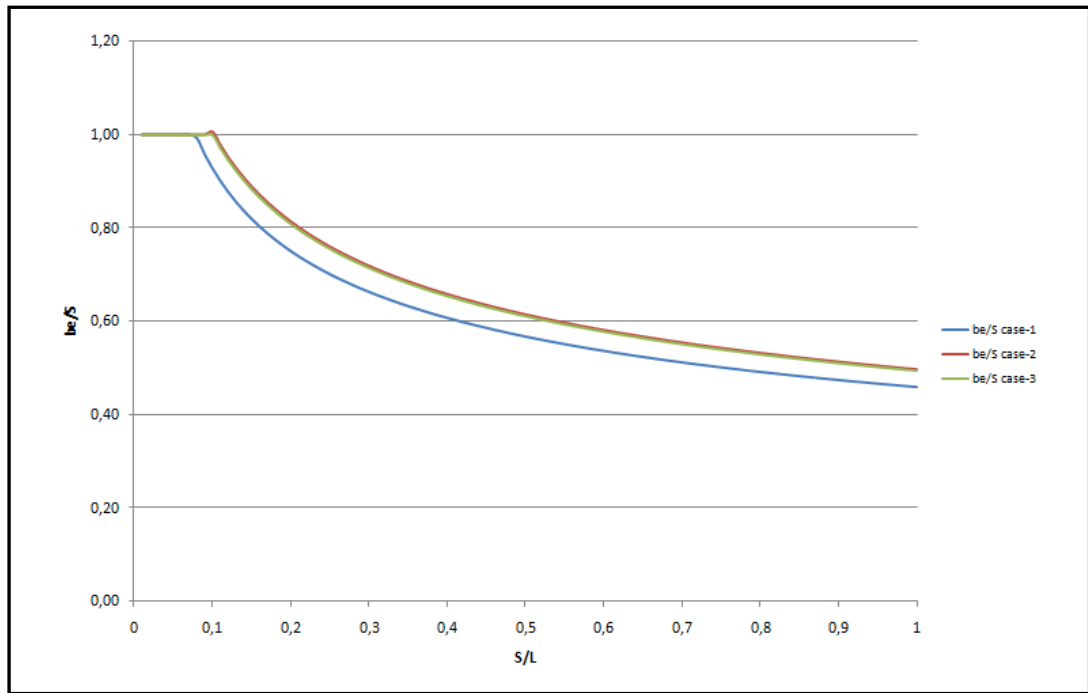
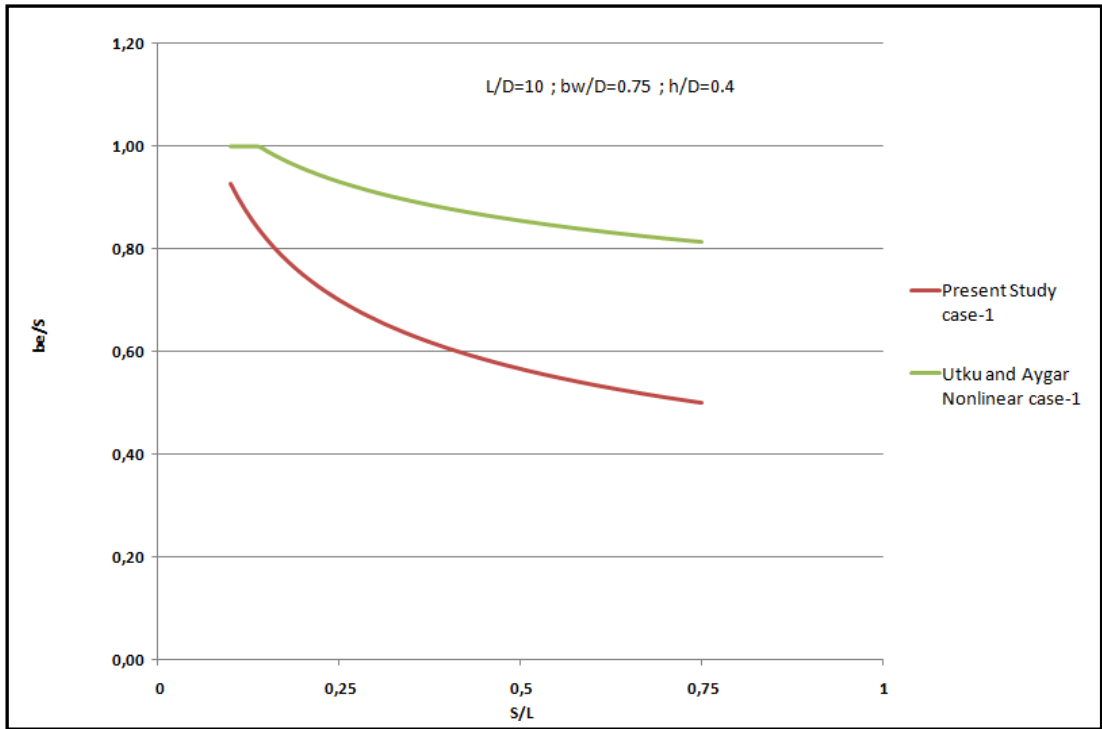
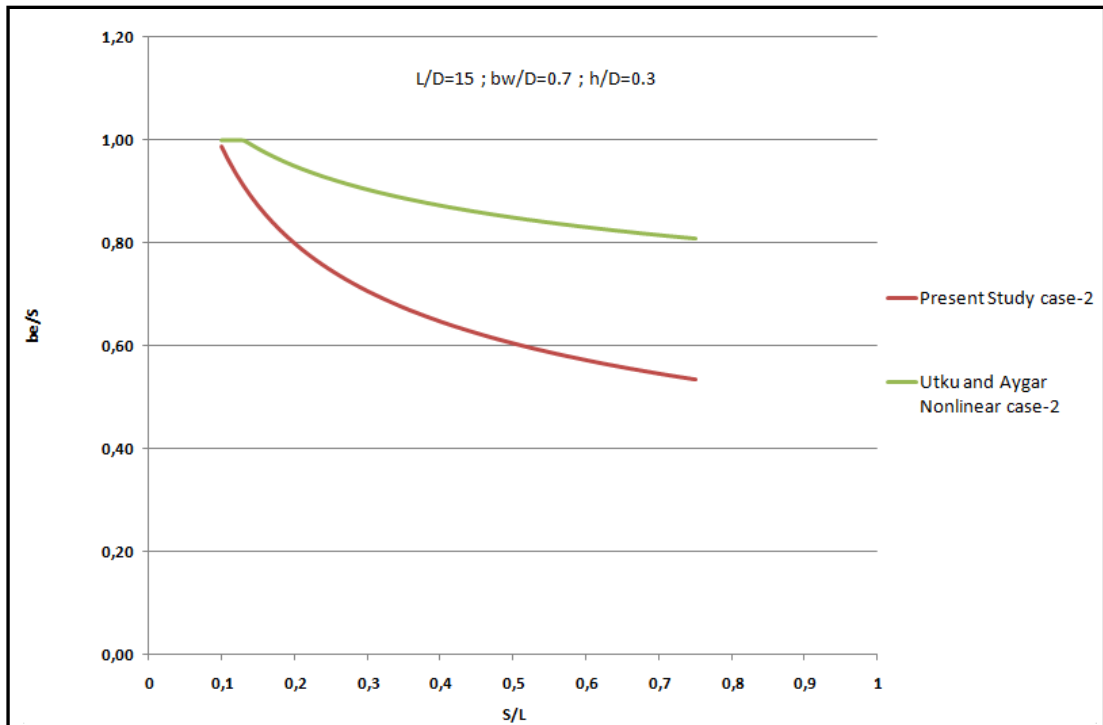


Figure 5.5 “S/L” versus “ $b_e/S$ ” for Case1, Case2 and Case3

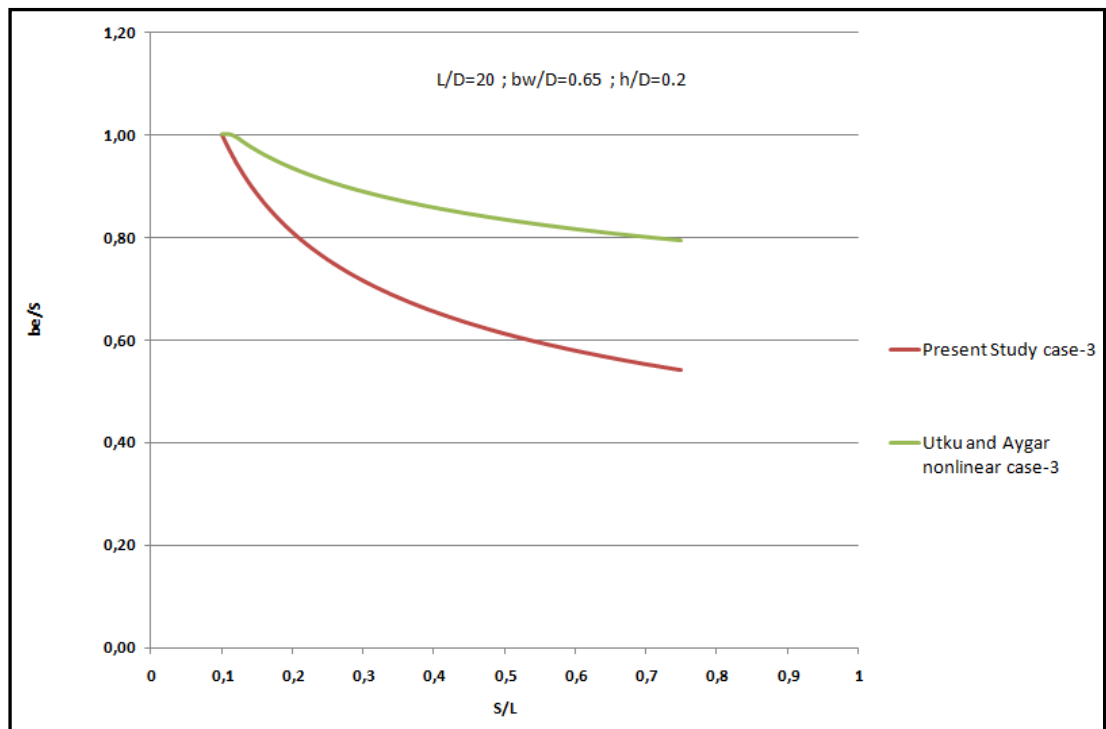
Figure 5.6 shows the comparison between the deflection based results of the present study and those obtained from stress criterion of Utku and Aygar (2002). It is observed that the results of the proposed equation for the uniformly distributed load case exhibit very good agreement with the results of stress criterion when the beam spacing is small. However, as the beam spacing increases the proposed equation has a tendency to produce conservative effective flange width values.



(a)  $L/D = 10$  ,  $b_w/D = 0.75$  ,  $h/D = 0.4$



(b)  $L/D = 15$  ,  $b_w/D = 0.7$  ,  $h/D = 0.3$



(c)  $L/D = 20$  ,  $b_w/D = 0.65$  ,  $h/D = 0.2$

Figure 5.6 Effective flange width based on stress criterion and deflection consideration (uniform loading)

## CHAPTER 6

### CONCLUSIONS

In this thesis, three-dimensional finite element analysis has been carried out on continuous T-beams to assess the effective flange width based on displacement criterion. The formulation is based on a combination of the elementary bending theory and the finite element method, accommodating partial interaction. Eight-node brick elements have been used to model the T-beams. The beam spacing, beam span length, total depth of the beam, the web and the flange thicknesses are considered as independent variables. Depending on the type of loading, the numerical value of the moment of inertia of the transformed beam cross-section and hence the effective flange width are calculated. The input data and the finite element displacement results are then used in a nonlinear regression analysis and two explicit design formulas for effective flange width have been derived. Comparisons are made between the proposed formulas and the ACI, Eurocode, TS-500 and BS-8110 code recommendations.

The following conclusions can be drawn from the results obtained in this study:

1. For the point load case, all codes give highly overestimated values for the effective flange width particularly for short and deep beams when the results are compared with the analyses based either on stress criterion or deflection consideration.
2. As the beam gets slender, this trend changes and smaller effective flange width values are obtained for increasing values of the beam

spacing. However, for all cases the recommendations given by Eurocode give overestimated results.

3. Using the curves developed from the proposed equations, it is observed that as the beam spacing  $S$  increases,  $b_e/S$  decreases. Moreover, for the same value of the beam spacing  $S$ , the ratio  $b_e/S$  increases as the span length  $L$  increases.
4. It is also concluded that the beam spacing  $S$  and the beam span length  $L$  affect the effective flange width more significantly than the other parameters.
5. For beams under a uniformly distributed load, it is found that the proposed formula gives underestimated results for stubby beams with respect to the code equations. However, as the beams get slender all codes yield very conservative assessments of  $b_e$  for uniformly distributed load case except for Eurocode which gives consistently overestimated results for all cases. For most of the beams under a uniform distributed load, Eurocode values of  $b_e/S$  are very close to unity.
6. Comparisons are made between the proposed deflection-based formulas and the formulation based on stress criterion. It is found that the results of the proposed equation for the uniformly distributed load case exhibit very good agreement with the results of stress criterion when the beam spacing is small. However, as the beam spacing increases the proposed equation has a tendency to produce conservative effective flange width values.

## REFERENCES

- Brendel, G., “*Strength of the Compression Slab of T-Beams Subject to Simple Bending*”, ACI Journal, Proceedings Vol.61, No.1, 57-75, Jan. 1964.
- Cook, R.D., Malkus, D.S. and Plesha, M.E., *Concepts and Applications of Finite Element Analysis*, Third Edition, John Wiley and Sons, New York. 1989.
- Ersoy, U., *Reinforced Concrete*, Middle East Technical University, Ankara, 1994.
- Fraser, D.J. and Hall, A.S., “*The Effective Flange Width of Integral T- and L-Beams*”, Civil Engineering Transactions, Vol.CE15, No.1-2, 74-76, 1973.
- Loo, Y.C. and Sutandi, T.D., “*Effective Flange Width Formulas For T-Beams*”, Concrete International: Design & Construction, Vol.8, No.2, 40-45, Feb. 1986.
- MacGregor, J.G. and Wight, J.K., *Reinforced Concrete: Mechanics and Design*, 4th Edition, Prentice Hall, New Jersey, 2005.
- Neter, J., Wasserman, W. and Whitmore, G.A., *Applied Statistics*, Fourth Edition, Allyn and Bacon, Massachusetts, 1993.

- Nilson, A.H. and Winter, G., *Design of Concrete Structures*, Eleventh Edition, McGraw-Hill Book Company, New York, 1991.
- Pecknold, D.A., “*Slab Effective Width for Equivalent Frame Analysis*”, ACI Journal, Proceedings Vol.72, No.4, 135-137, Apr. 1975.
- Timoshenko, S.P. and Goodier, J.N., *Theory of Elasticity*, McGraw Hill Book Company, New York, 1970.
- Utku, M. and Aygar, A., “*Investigation of Effective Flange Width Formulas for T-Beams*”, Proceedings of the Sixth International Conference on Computational Structures Technology, Paper 13, Prague, Czech Republic, 4- 6 September 2002.
- Betonarme Yapıların Hesap ve Yapım Kuralları*, TS500, Türk Standardları Enstitüsü, Nisan 1984.
- Building Code Requirements for Reinforced Concrete Buildings*, ACI-318-95, American Concrete Institute, Michigan, 1995.
- Eurocode 2: Design of Concrete Structures-Part 1: General Rules for Buildings*, 1991.
- SAP 2000 Advanced V.11.0.0*, Computers and Structures, Inc., Berkley, California, 1976 - 2007.
- Statistical Package for the Social Sciences for Windows*, Release 15.0.0., 2006.